



**HAL**  
open science

## Surface Modification of Metallic Catalysts for the Design of Selective Processes

Dan Wu, Dandan Han, Wenjuan Zhou, Stéphane Streiff, Andrei Khodakov,  
Vitaly Ordonsky

► **To cite this version:**

Dan Wu, Dandan Han, Wenjuan Zhou, Stéphane Streiff, Andrei Khodakov, et al.. Surface Modification of Metallic Catalysts for the Design of Selective Processes. *Catalysis Reviews: Science and Engineering*, 2022, pp.1-47. 10.1080/01614940.2022.2079809 . hal-03861660

**HAL Id: hal-03861660**

**<https://hal.science/hal-03861660>**

Submitted on 20 Nov 2022

**HAL** is a multi-disciplinary open access archive for the deposit and dissemination of scientific research documents, whether they are published or not. The documents may come from teaching and research institutions in France or abroad, or from public or private research centers.

L'archive ouverte pluridisciplinaire **HAL**, est destinée au dépôt et à la diffusion de documents scientifiques de niveau recherche, publiés ou non, émanant des établissements d'enseignement et de recherche français ou étrangers, des laboratoires publics ou privés.

# Surface Modification of Metallic Catalysts for the Design of Selective Processes

Dan Wu<sup>a,b,c</sup>, Dandan Han<sup>d</sup>, Wenjuan Zhou<sup>b</sup>, Stephane Streiff<sup>b</sup>, Andrei Y. Khodakov<sup>a\*</sup> and Vitaly V. Ordomsky<sup>a\*</sup>

*<sup>a</sup>Univ. Lille, CNRS, Centrale Lille, ENSCL, Univ. Artois, UMR 8181 – UCCS – Unité de Catalyse et Chimie du Solide, F-59000 Lille, France;*

*<sup>b</sup>Eco-Efficient Products and Processes Laboratory (E2P2L), UMI 3464 CNRS-Solvay, 201108 Shanghai, People's Republic of China;*

*<sup>c</sup>School of Chemical Engineering, Zhengzhou University, Zhengzhou, 450001, People's Republic of China*

*<sup>d</sup>College of Science, Henan Agricultural University, Zhengzhou, Henan 450002, People's Republic of China*

Corresponding authors: Vitaly V. Ordomsky, Email: [vitaly.ordomsky@univ-lille.fr](mailto:vitaly.ordomsky@univ-lille.fr);  
Andrei Y. Khodakov, Email: [andrei.khodakov@univ-lille.fr](mailto:andrei.khodakov@univ-lille.fr)

Dan Wu, Andrei Y. Khodakov, and Vitaly V. Ordomsky conceived the ideas for this review. All authors contributed to the writing of the review. Dan Wu and Dandan Han prepared the draft with the help of Wenjuan Zhou and Stephane Streiff. The manuscript was directed and revised by Andrei Y. Khodakov, and Vitaly V. Ordomsky.

Fine-tuned interaction between reacting molecules and metal surface is of great importance in heterogeneous catalysis for the design of highly selective processes. Conventional strategies based on adjusting the intrinsic catalyst properties such as particle size, metal-support interaction and morphology suffer from complicated and time-consuming synthetic procedures. Recently, the modification of metal nanoparticles with non-metallic promoters has been demonstrated as an effective tool to regulate the interfacial environment of metallic catalysis. Herein, we will give an overview of recent progress in this area. A general analysis will be proposed about the electronic, steric effects and new functionalities imposed by non-metallic promoters of metal catalysts. The potential for the selectivity enhancement of the promoted metal catalysts in various industrially important reactions is discussed.

**Keywords:** Heterogeneous catalysis; Surface modification; Steric effect; Electronic effect; Bifunctionality

## **1. Introduction**

### ***1.1. General introduction***

Due to the high density of active sites, stability and recyclability, metal nanoparticles are widely used in industrial catalytic processes such as hydrogenation, oxidation, amination, cascade reactions, and so on<sup>1-6</sup>. However, one of the main challenges in metal catalysis is insufficient selectivity to target products, which requires additional energy consumption for separation and recycling of by-products. It causes numerous environmental problems and increases the technological costs. The insufficient selectivity is a result of low specificity of interaction between the active site and reacting molecules leading to undesirable side reactions.

On the other side, industrial processes require catalysts with uniform and well-defined properties, especially for fine chemical manufacturers. Various reactions towards different products proceed on the surface of metal nanoparticles with different environments<sup>7-15</sup>. The parameters that affect the catalytic properties of metal nanoparticles include electronic structure, surface texture, metal-support interaction, particle size and morphology, and so on. Normally, these parameters are well-optimized for commercial catalysts. For this reason, the design of new catalytic materials based on the existing commercial catalysts via their modification with non-metallic promoters is an attractive and economic way. However, in most cases, screening of the existing industrial catalysts with various metals, loadings, and supports in new catalytic processes does not give satisfactory results because of insufficient selectivity.

Inspired by enzymatic and homogeneous organometallics catalysis, tuning the electronic and steric effects of metal nanoparticles by organic ligands such as polymers, amines, thiols, halogens etc has attracted a lot of attention<sup>16-21</sup>. Surface modification with

non-metallic promoters avoids the complex catalyst synthesis procedures and could be easily adapted to the existing commercial catalysts.

A literature analysis using Web of Science indicates an exponential growth of number of publications dedicated to the surface modification of metallic catalysts (**Figure 1**). Most recently, a large number of works are devoted to the selectivity control in the hydrogenation of biomass-derived platforms by modification of the metal catalysts with non-metallic promoters such as thiols and halogens<sup>22-32</sup>.

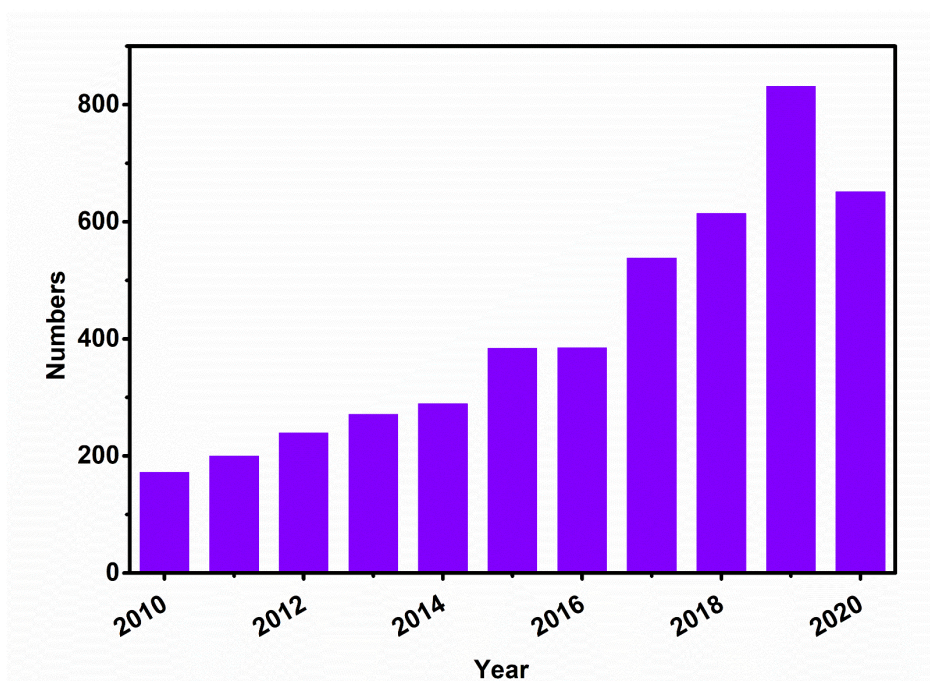


**Figure 1.** Numbers of publications related to surface modification of heterogeneous metal catalysts. From Web of Science<sup>TM</sup> all collections, Booleans: TS=(metal AND heterogeneous catalysis AND (ligand OR stabilizer OR modifier OR capping agent OR surfactant OR selective poisoning OR promoters) )

Catalysis over metal surfaces involves molecule adsorption, diffusion, reaction, and desorption<sup>33-38</sup>. The reactant molecules firstly diffuse from the reactant phase to the catalytic interface. In this case, a steric effect might be introduced by the promoters,

which tune the configuration and orientation of the molecules approaching the metal surface. Moreover, the molecular affinity between the surface and reactant molecules will determine the concentration of reactant molecules on the catalyst. For example, hydrophobic promoters endow quick diffusion and enhanced adsorption of hydrophobic reactants, while hydrophilic promoters favor diffusion and adsorption of hydrophilic reactant molecules. When the orientations of the reactant molecules have been pre-adjusted, they can readily adsorb in a specific configuration on the metal surface. In this case, the nature of active sites will determine the activation and transformation of the reactant molecules. The electronic effects and bifunctionality introduced by promoters will tune the reaction activity and selectivity. Usually, these effects are strongly interconnected with each other (**Figure 2**).

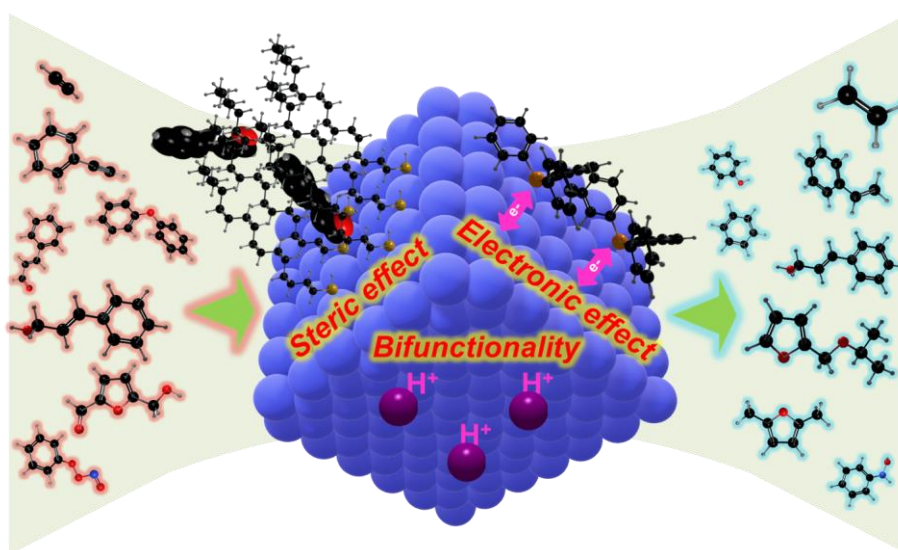


**Figure 2.** Multifunctional effects of surface modification in the design of metal catalysts.

The scope of this review covers steric, electronic and bifunctionality effects in the metal catalysts (e.g. Pd, Pt, Au, Ni, Cu, Co, et al.) modified with non-metallic promoters (polymers, thiols, amines, halogens, et al.). The common feature of these metals is that they have incompletely filled *d*-orbitals. These metals are characterized by a relatively

low energy transitions between possible oxidation states. They are commonly used as catalysts for industrial production of chemicals.

### 1.2. Different non-metallic promoters

Numerous non-metallic promoters have been used for modification of metallic catalysts. The representative promoters/metal combinations and the corresponding reactions are summarized in **Table 1**. In this review, the non-metallic promoters are divided into five categories: (1) Heavy molecules, e.g. polyvinylpyrrolidone (PVP), polyvinyl alcohol ((PVA), polyethylene (PE), 4-ethynytoluene, 1,2-di-p-tolyethyne, and HDDMA<sup>39-50</sup>; (2) N-based compounds, e.g. long-chain alkylamines, alkanolamines, ethylenediamine, quinoline, N-heterocyclic carbenes<sup>51-69</sup>; (3) P-base compounds, e.g. triphenylphosphine<sup>70-78</sup>; (4) S-base compounds, e.g. alkanethiols, diphenyl sulfide, H<sub>2</sub>S<sup>79-102</sup>; (5) Halogens-based compounds, e.g. ethyl iodide, dichloromethane, bromobenzene<sup>103-118</sup>. In some cases, these molecules not only act as promoters but also as capping agents for the synthesis of metal nanoparticles<sup>119-122</sup>.

**Table 1.** Summary of the representative promoters in various catalytic systems

Category	Promoters	Metals	Reactions	Ref.
Heavy molecules	Polyvinylpyrrolidone (PVP)	Au	Hydrogenation of <i>p</i> -chloronitrobenzene and cinnamaldehyde	155
	PVP	Pd	Nitrite hydrogenation	156
	Polyvinyl alcohol (PVA)	Pd	Nitrite hydrogenation	156
	Polyethylene glycol (PEG)	Pd	Direct synthesis of H <sub>2</sub> O <sub>2</sub>	102
	Polyacetylene	Pd	Hydrogenation of styrene and nitrobenzene	40
	Poly(allylamine)	Pd	Formic acid decomposition	47
	Terminal and internal alkyne	Ru	Styrene hydrogenation	39
	Hexadecyl trimethyl ammonium bromide (CTAB)	Au	Hydrogenation of <i>p</i> -chloronitrobenzene and cinnamaldehyde	157
	Sodium S-dodecylthiosulfate	Pd	Isomerization and hydrogenation of allyl alcohol	94
	Hexadecyl (2-hydroxyethyl)	Pd	Semi-hydrogenation of alkynes	53

	dimethyl ammonium dihydrogen phosphate (HHDMA)			
	HHDMA	Pt	Hydrogenation of nitroarene	53
	HHDMA	Pt	Hydrogenation of levulinic acid	158
	HHDMA	Pd	Hydrogenation of benzonitrile and benzaldehyde	62
	HHDMA	Pt	Semi-hydrogenation of alkynes	58
	HHDMA	Ni	Direct synthesis of H <sub>2</sub> O <sub>2</sub>	144
N-based compounds	Ethylenediamine	Pt	Hydrogenation of nitroaromatics	60
	Long-chain alkylamines	Pt <sub>3</sub> Co	Hydrogenation of cinnamaldehyde	69
	N-heterocyclic carbenes (NHCs)	Pd	Hydrogenolysis of bromobenzene	65
	l-proline (PRO)	Pt	Hydrogenation of acetophenone	159
	PRO	Pt	Asymmetric hydrogenation of methylacetoacetate	52
	Oleylamine, and trioctylphosphine	Ni	Hydrogenation of furfural	160
	NHCs	Au	Cycloisomerization of alkynyl amines to indoles	59
	Ethylenediamine	Ni	Hydrogenative coupling of nitrobenzene	161
	$\alpha$ -Amino acids	Pt	Hydrogenation of $\beta$ -keto esters	162
	Aspartic acid	Pt	Hydrogenation of $\alpha$ , $\beta$ -unsaturated aldehydes	163
	Piperazine	Au	Semi-hydrogenation of alkynes	68, 164
	Primary alkylamines	Pt	Semi-hydrogenation of alkynes	54
P-base compounds	Triphenylphosphine (PPh <sub>3</sub> )	Pd	Hydrogenation of acetophenone, phenylacetylene, and nitrobenzene	73
	PPh <sub>3</sub>	Pd	Acetylene hydrogenation	88
	Trioctylphosphine (TOP)	Ni	Hydrogenation of furfural	160
	Phosphine ligand TOP	Rh	Hydrogenation of phenylacetone	78
	TOP	Pd	Acetylene hydrogenation	77
	Secondary phosphine oxides (SPOs)	Ru	Hydrogenation of aromatics	75
	Tert-butyl (naphthalen-1-yl) phosphine oxide	Au	Hydrogenation of substituted aldehydes	70
	Tricyclohexylphosphine (PCy <sub>3</sub> )	Cu	Hydrogenation of 1-phenyl-1-propyne	76
	NH <sub>4</sub> H <sub>2</sub> PO <sub>2</sub>	Pd	Acetylene hydrogenation	74
	Phosphonic acids	Pt	Hydrodeoxygenation of aromatic alcohols and phenolics	29
S-base compounds	SPL8-4 and SPL8-6	Pd	Semi-hydrogenation of alkynes	165
	n-Alkanethiol	Pd	Hydrogenation of 1-epoxy-3-butene	81
	1,6-Dithiolhexane	Pt	Hydrogenation of nitroarenes	93
	Diphenyl sulfide	Pd	Acetylene hydrogenation	100
	3,4-Difluorothiol Na <sub>2</sub> S	Pd	Semi-hydrogenation of internal alkynes	101
		Pd	Semi-hydrogenation of alkynes	97
	1-Dodecanethiol	Pd	Hydrogenation of polyunsaturated fatty acid	99
	Phenyl sulfide	Pd	Acetylene hydrogenation	88
	1-Octadecanethiol and benzene-1,2-dithiol	Pd	Hydrogenation of furfural	86
	1-Dodecanethiol	Au	n-Butanolysis of dimethylphenylsilane	87
	Diphenyl Sulfide	Pd	Hydrogenation of <i>p</i> -Chloronitrobenzene	166
3-Phenyl-1-propanethiol	Pt	Hydrogenation of cinnamaldehyde	80	



	1-Octadecanethiol and 1-adamantanethiol	Pd	Acetylene hydrogenation	82
	1-Dodecanethiol	Pt	Hydrogenation of crotonaldehyde	91
	1-Octadecanethiol and 1-adamantanethiol	Pd	Hydrogenation of furfural	84
Halogen-based compounds	Bromide	Pd	Direct synthesis of H <sub>2</sub> O <sub>2</sub>	167
	Iodine	Ni	Hydrogen evolution reaction	113
	Iodide	Pd	Reductive Etherification of Carbonyl Compounds	108
	Bromide	Pd	Hydrogenation of aromatic ethers	116
	Fluorine	Cu	Electrocatalytic reduction of CO <sub>2</sub> to ethylene and ethanol	168
	Bromine	Pd	Hydrodeoxygenation of 5-hydroxymethylfurfural	106
	Bromine	Ru	Hydrogenolysis of aryl ethers	109
	Chlorine	Cu	Electrocatalytic reduction of CO <sub>2</sub> to C <sub>2</sub> <sup>+</sup>	169
	Iodide	Cu	Electrocatalytic reduction of CO <sub>2</sub> to C <sub>2</sub> <sup>+</sup>	170

Usually, the promoters anchor on the metal surface via their “headgroups”. There are two kinds of interactions between promoters and metal surfaces. The first one is covalent bonding (mostly via coordination bonds), and the second one involves non-covalent interactions (such as van der Waals forces and electrostatic interactions).

The headgroups usually contain heteroatoms e.g. nitrogen, phosphorus, oxygen and sulfur, or electron-donating functional groups e.g. -C=C-, and -C≡C-. These headgroups coordinate to the metal surface by charge-transfer interactions. Polymeric promoters without electron-donating groups are attached to the metal surface via van der Waals forces. Ionic, amphiphilic surfactants such as HHDMA and CTAB absorb over the metal surface via their ionic headgroups and the strong electrostatic interactions with the metallic surface play a dominant role in promoter immobilization on the surface.

### 1.3. Stability of promoters

The presence of promoters on the metal surface creates steric, electronic and bifunctionality effects, which could enhance the catalytic properties of metal catalysts. The stability of promoters on the metal surface is an important issue for the catalyst design, catalyst reusability and manufacturing of clean chemical products, which are non-polluted with the promoters<sup>123-125</sup>.

Due to the high electron-donating ability, coordination bonds formed by heteroatoms such as oxygen, nitrogen, sulfur, phosphorus and halogens with the catalyst surface are usually more stable than the  $-C=C-$  and  $-C\equiv C$  counterparts<sup>14, 126</sup>. The electrostatic interactions between ionic, amphiphilic surfactants such as HHDMA and metal surfaces are also strong and avoid their desorption during several reaction cycles.

It is worth noting, the stability of the promoters is affected by the reaction conditions such as water content, solvent properties,  $H_2$  pressure, temperature and so on. Specifically, heavy molecules as ionic surfactants may suffer from leaching problems, however, they could be more stable in low-temperature gas-phase reactions<sup>74</sup>. Thus, the use of surface promoters bearing strong coordination to the catalyst surface and often containing chelating groups (e.g. thiolates, diamines) is usually required for the design of stable catalysts.

#### ***1.4. Direct preparation or post modification?***

The strategies for anchoring non-metallic promoters on the surface of metal nanoparticles can be summarized in two groups. The first one is direct-preparation, in which the non-metallic promoters are mixed with the metal precursors during the catalyst synthesis and after reduction of the metal precursors, the promoters directly localize on the surface of metal nanoparticles<sup>20, 68, 127-132</sup>. The second strategy is post-modification. In this strategy, the non-metallic promoters are anchored on the metal surface by post-treatment of the earlier prepared catalysts<sup>41, 106, 108, 109</sup>.

Direct-preparation is applied usually for the synthesis of ligand-protected colloidal metal nanocrystals (MNCs), where the promoters normally act as capping or protecting agents. They confine the over-growth and aggregation of MNCs<sup>133</sup>. This approach is known to produce high-quality MNCs with tunable size and shape, narrow size dispersion and high crystallinity. Generally, MNCs with capping agents exhibit lower activity than

the bare metal nanoparticles. This phenomenon is mainly due to the partial blockage of active sites by capping agents. However, it was recently found that the capping agent could endow some abnormally catalytic properties to MNPs<sup>43, 69</sup>. Thus, the role of the capping agent on the catalytic properties of MNCs is more complex. Direct-preparation of MNCs with different capping agents has been intensively reported and reviewed<sup>171-174</sup>. Some of them focused on the utilization of capping agents in heterogeneous catalysis.

Due to the easy realization and close to industrial application, post-modification has been attracting more and more attention. Post-modification was extensively used to modify supported metal catalysts and colloidal metal NPs<sup>40</sup>. Various post-modification methods have been reported: (1) On-metal-surface polymerization<sup>41, 110</sup>; (2) Self-assemble monolayers (SAM)<sup>80-83</sup>; (3) Atomic element decoration<sup>106, 108, 109, 113</sup>. On-metal-surface polymerization is used when the promoters have the polymerizable functional groups and the polymerization could be initiated by the metal surface. The formation of self-assemble monolayers requires the promoters to have the long-alkane tails. And the atomic element decoration happens, when the metal nanoparticles interact with sulfur and halogens.

## **2. Role of the promoters**

Coordination of non-metallic promoters on the active metal surface results in several effects on the catalytic process. First of all, the presence of promoters can change the structural geometry as well as the spatial arrangement of the catalyst surface. The on-surface change involves blocking the active sites, which prevents adsorption of reactant molecules as well as limits the diffusion of intermediates on the surface. The outer-surface changes derive from the promoters, which have long and bulky “tails” such as the amphiphilic modules. These tails can interact with the reactant molecules via creating steric space hindrances and introducing weak interactions (e.g. van der Waals forces,

hydrogen bonding, aromatic ring stacking), when the reactant molecules approach the catalyst surface<sup>14, 125</sup>. Besides the steric effects, the coordination of promoters will change the electronic structure of metal surface, e.g. the Fermi core level<sup>134</sup>. Understanding the electronic effects could be more difficult compared to the steric effects. The electronic effect is relevant to changing the electronic structure of surface metal atoms and the intrinsic activity of surface sites<sup>60</sup>. During the real catalytic process, both the steric and electronic effects can impact the catalytic behavior. Identification of steric and electronic effects and their contributions to catalysis is therefore the primary task. In addition to steric and electronic phenomena, the non-metallic promoters can also introduce new types of active sites in the metallic catalysts. Bifunctional catalysts and sites derived from non-metallic promoters attract a lot of attention<sup>135</sup>. Notably, bifunctional catalysts produced by the promotion of metallic catalysts with non-metallic promoters possess proximate metal-acid or metal-base sites, which are important for many catalytic processes.

### **2.1. Steric effects**

The steric effects strongly affect the accessibility of reactant molecules on the metal surface. The steric effects can be more significant for large molecules<sup>41</sup>. Numerous papers have ascribed to steric effect the abnormal catalytic behavior after the modification, but only a few of them focus on understanding the interaction mechanism between the reactants and promoters. The understanding of the way how the steric effects change the behavior of reactant molecules is important, because it can guide the rational design of the smart catalytic surfaces.

The steric effect can have different nature and can involve different promoters. For example, the non-metallic promoters could be polymers, N-, S- based organic molecules. The presence of steric effects usually decreases the overall activity and changes the

selectivity. Several mechanisms have been proposed to explain the abnormal catalytic performance by comparing it with the non-modified catalyst. These mechanisms involve on-surface effects of (1) selective sites blocking<sup>49, 109</sup>, (2) active sites isolation<sup>14, 101</sup>, and outer-surface effects of (3) surface wettability<sup>83, 102</sup>, (4) molecular orientation<sup>69, 99</sup> (5) surface molecular imprinting<sup>136</sup> (**Figure 3**). Let us discuss them in greater detail.

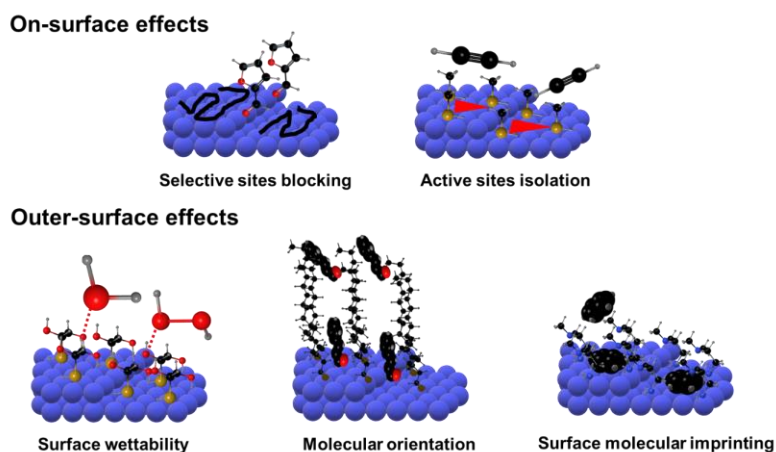


**Figure 3.** Different kinds of steric effects: On-surface effects of selective sites blocking, active sites isolation, outer-surface effects of surface wettability, molecular orientation and surface molecular imprinting.

### 2.1.1. Selective site blocking

Polymer modifiers are often used for selective blocking of active sites. Sebastiano et al. have reported the selectivity control in the palladium-catalyzed alcohol oxidation through selective blocking with PVA of the Pd (111) facets, which were active in the decarboxylation reaction of benzaldehyde<sup>49</sup>. The supported Pd nanoparticles protected by PVA showed an improved selectivity toward benzaldehyde in the benzyl alcohol aerobic oxidation compared with the unprotected Pd nanoparticles. This enhancement resulted from a lower rate of benzaldehyde decarboxylation.

The alkyne modified ruthenium nanoparticles have been synthesized and compared with the non-modified counterparts for selective hydrogenation of styrene by Zhang et al

<sup>39</sup>. As illustrated in **Figure 4**, two different kinds of alkynes have been used, terminal alkyne e.g. 4-ethynyltoluene and internal alkyne e.g. 1,2-di-p-tolyne. The alkyne showed different adsorption configurations on the surface of Ru (0001). The terminal alkyne adsorbs strongly in comparison with internal alkyne with the Ru=C=HCH- interfacial bonds. Internal alkyne adopted an  $\eta^2$  side-on configuration and formed a  $\delta$ - $\pi$  covalent bond. It means that the internal alkyne blocked the bridge sites, while the terminal alkyne blocked the hole sites. The selective blocking of active sites leads to different catalytic results. Thus, Ru nanoparticles capped with terminal alkynes exhibited catalytic activity towards hydrogenation of both the C=C and phenyl rings of styrene, while Ru nanoparticles capped with internal alkynes exhibited high activity towards the hydrogenation of the C=C bonds only. This discrepancy has been caused by the different sites needed for the hydrogenation of C=C bonds and phenyl rings.

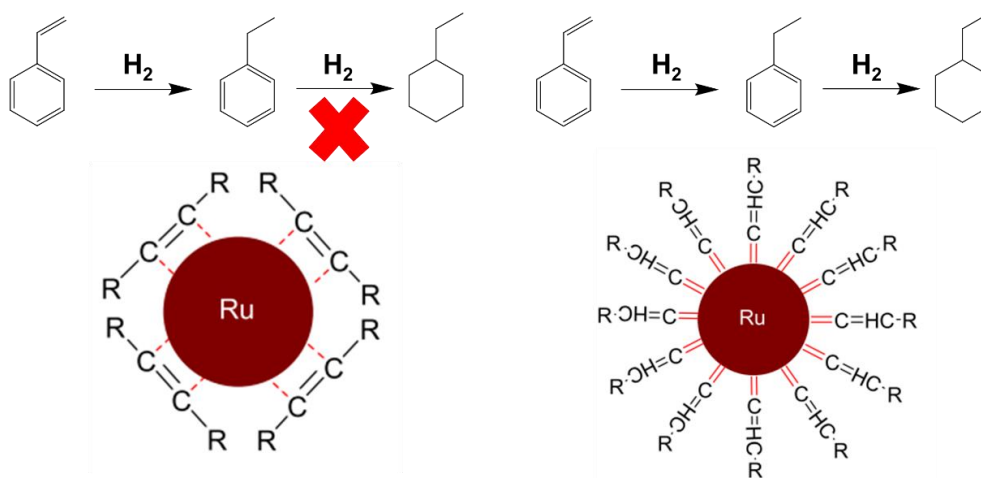


**Figure 4.** Adsorption configurations of terminal alkyne and internal alkyne on Ru nanoparticles for selective hydrogenation of styrene <sup>39</sup>.

The sulfur-based modifiers like thiols have been extensively used as selective blocking agents for metal catalysts <sup>83, 125</sup>. For example, the reaction pathways for furfural hydrogenation have been well-controlled on supported Pd catalysts with self-assembled thiols monolayers <sup>84</sup>. As shown in **Figure 5**, two different thiol molecules: linear 1-

octadecanethiol ( $C_{18}$ ) and bulky 1-adamantanethiol (AT) were used to modify the Pd surface for catalytic hydrogenation of furfural. The  $C_{18}$  thiols selectively block the terrace sites, while AT thiols sparsely block the terraces, edges, and corners sites without discrimination. It means that the catalyst modified by the  $C_{18}$  thiol has the only accessible sites at the particle edges and steps, whereas the AT modified catalyst provides access for the reacting molecules only to the sites on the particle terraces. The accessibility of different active sites results in different catalytic behaviors in the furfural hydrogenation. Pd modified by  $C_{18}$  thiol showed higher activity in the hydrogenation and deoxygenation of carbonyl groups, while AT modified Pd exhibited decarbonylation of aldehyde group and hydrogenation of furan rings.

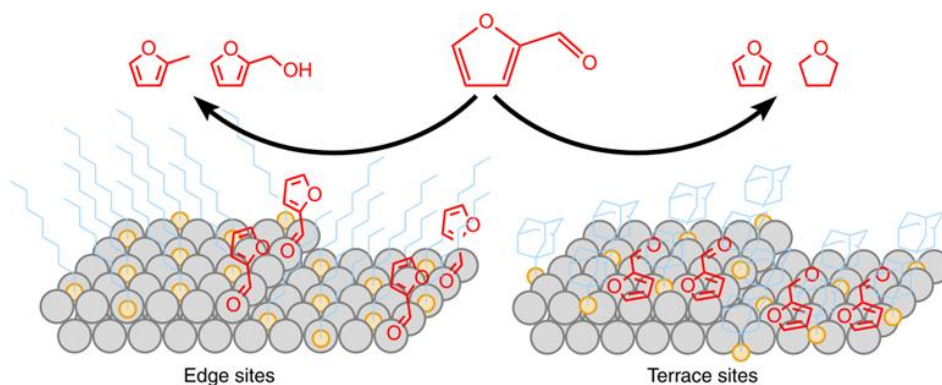


**Figure 5.** Proposed adsorption mechanism of furfural on  $C_{18}$  and AT modified catalysts

84

Recently, our group has modified the Ru/C catalyst with bromobenzene and prepared partially brominated Ru nanoparticles for hydrogenolysis of aryl ether bonds without hydrogenation of the aromatic rings<sup>109</sup>. The enhanced catalytic performance was ascribed to the selective blocking of the terrace sites by Br atoms which are active sites for benzene ring hydrogenation. As demonstrated by the CO-FTIR spectroscopy (**Figure 6**), adsorption of CO on the initial Ru nanoparticles leads to a peak at  $1998\text{ cm}^{-1}$  ascribed

to CO adsorbed on the edge and corner sites, and another peak at  $1877\text{ cm}^{-1}$  due to CO adsorbed on the terrace sites. However, after selective poisoning by Br, the peak at  $1887\text{ cm}^{-1}$  disappeared, indicating the selective poisoning of terrace sites by Br. The selective deposition of Br atoms on the terrace sites (continuous sites) prevents the adsorption of phenyl rings, thus hindering aromatic ring hydrogenation.

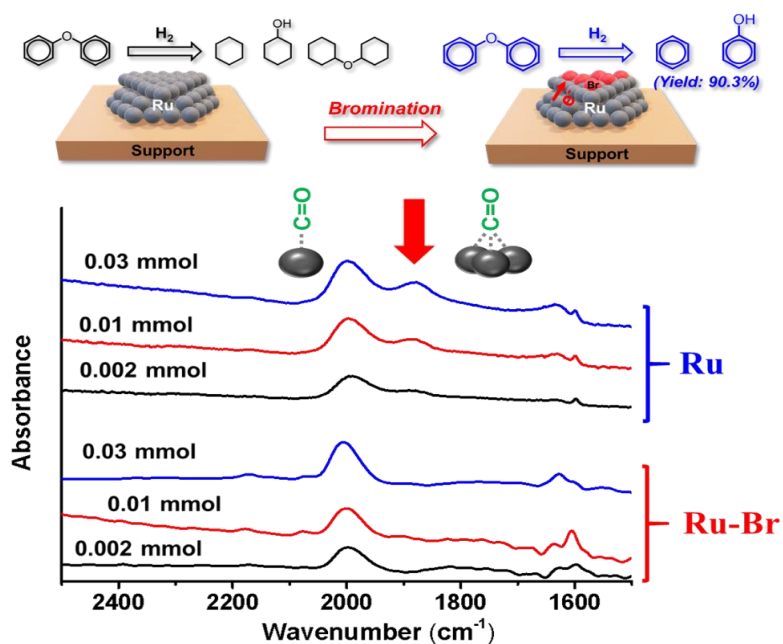


**Figure 6.** Selective poisoning of terrace sites over Ru nanoparticles by Br for selective hydrogenation of diphenyl ether to benzene and phenol<sup>109</sup>.

### 2.1.2. Active sites isolation

In heterogeneous catalysis, the reactant molecules are adsorbed and activated on the metal surface. This process may require the participation of multiple metal atoms on the surface. The active site isolation reduces the size of active assemblies and results in a change of the catalytic behavior for some specific reactions<sup>93, 98, 101</sup>. One of the important features in catalysis is selective activation of terminal functional groups. The terminal part of a molecule can much more easily access the active site than the internal part. For example, when the cobalt nanoparticles were treated with 1-butanol at a high temperature, the polymeric carbon species were produced on the cobalt surface. The carbon species



may introduce a strong steric effect on the amination of 1-butanol to 1-butyl amine<sup>41</sup>. The hydrogenation of internal imine groups has been suppressed because of the steric effect (Figure 7).

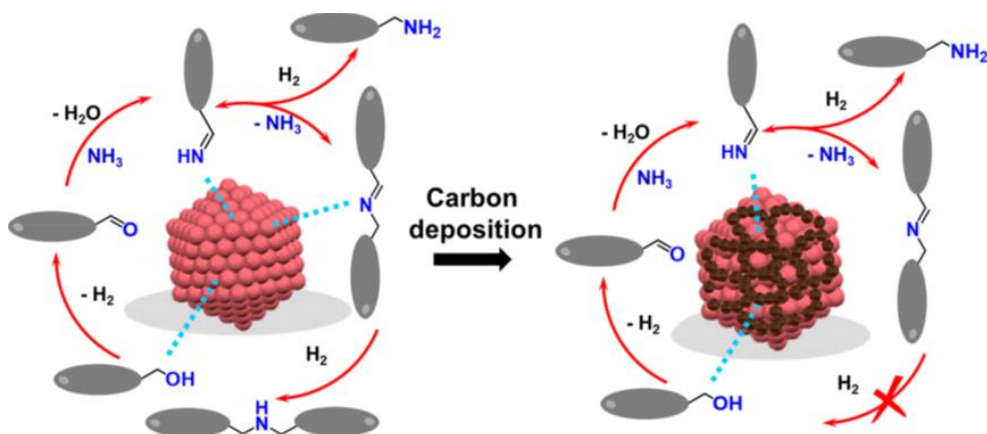


**Figure 7.** Prevention of the reaction of the internal imine groups by a steric effect over Co catalysts with deposited carbon species<sup>41</sup>.

Partial hydrogenation of alkynes to alkenes is the most widely studied model reaction over modified metal catalysts<sup>137</sup> due to the industrial significance of this reaction towards the manufacturing of polymers, pharmaceuticals, vitamins, and fragrances. This process suffers from over-hydrogenation to alkanes<sup>138, 139</sup>. Davide et al. have reported a nanostructured Pd<sub>x</sub>S (e.g. Pd<sub>3</sub>S and Pd<sub>4</sub>S) phase with controlled crystallographic orientation exhibiting unparalleled performance in the semi-hydrogenation of alkynes in the liquid phase<sup>97</sup>. The presence of sulfur defined a structure integrating spatially-isolated palladium trimers, which were responsible for the superior catalytic performance. DFT calculations were performed to gain insight into the comparative reaction mechanisms over Pd and Pd<sub>x</sub>S. As shown in Figure 8, the Pd<sub>x</sub>S catalysts have a lower ethene desorption energy than needed for its further hydrogenation and a higher energy barrier for oligomerization. DFT analysis demonstrated the advantage of Pd<sub>3</sub> site isolation and explained the high selectivity to ethene on the Pd<sub>x</sub>S catalyst.

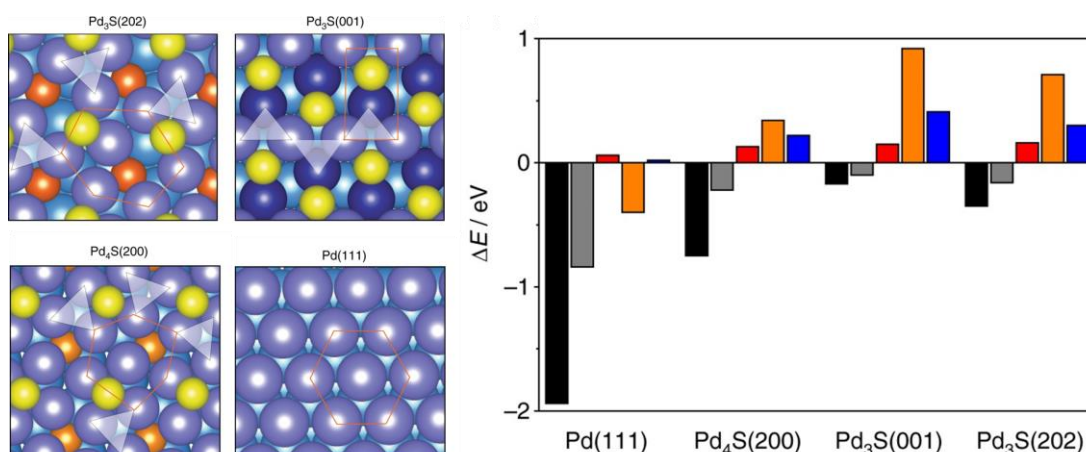


**Figure 8.** DFT analysis for the hydrogenation of acetylene over Pd (111), Pd<sub>4</sub>S (200), Pd<sub>3</sub>S (001) and Pd<sub>3</sub>S (202). Left: Structural resemblance of Pd<sub>3</sub>S and Pd<sub>4</sub>S to pristine Pd surfaces; Right: Energy differences: HCCH adsorption (black bars), H<sub>2</sub>CCH<sub>2</sub> desorption (gray bars), and the difference in activation energy between H<sub>2</sub>CCH<sub>2</sub> (ethene) and HCCH<sub>3</sub> (ethylidene) formation (red bars), H<sub>2</sub>CCH<sub>2</sub> desorption and H<sub>2</sub>CCH<sub>3</sub> formation (orange bars), and for oligomerization (blue bars).

The Pd NanoSelect catalyst developed by BASF is prepared by a chemical reduction method employing HHDMA as a reducing agent, stabilizer, and modifier consequently<sup>53</sup>. This catalyst consists of palladium nanoparticles of 5 ~ 8 nm supported on carbon or titanium silicate that exhibit alkene selectivity comparable to that provided by Lindlar's catalyst in the semi-hydrogenation of alkynes. Pérez-Ramírez et al. have studied the promotion effect of HHDMA on the Pd NanoSelect catalyst by experimental and theoretical methods<sup>20</sup>. According to DFT calculations, HHDMA is adsorbed rigidly over the Pd surface and restricts the accessibility of the substrate to the active sites of the catalyst (forming cavities with the elliptical shape), providing exceptional performance for the hydrogenation of terminal alkynes but low activity for disubstituted and bulky alkynes (Figure 9). Meanwhile, the presence of rigidly adsorbed HHDMA reduced the hydride coverage on the Pd surface via electronic effects.

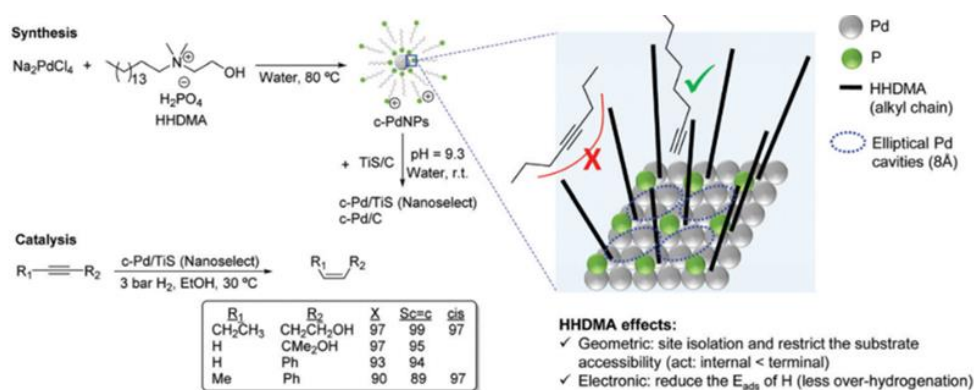


**Figure 9.** Illustration of the preparation of Pd catalyst capped with HHDMA <sup>53</sup>.

### 2.1.3. Surface wettability

Wetness affinity represents an intermolecular interaction between the tails of the promoters and reactant molecules. It is an outer-surface effect and depends on the wetness nature of the tails of promoters and the reactant molecules. Normally, the hydrophilic and hydrophobic properties of the promoters are used to explain the wetness affinity in catalysis <sup>140-142</sup>. The hydrophobic affinity is relevant to the presence of alkane chains, while the hydrophilic affinity is associated with the polar groups, which might form H-bonds with reactants. The key role of wetness affinity is to control the concentration of molecules on the catalyst surface. For example, promoters with hydrophobic long alkane chains can concentrate the hydrophobic reactant molecules on the catalyst surface and accelerate the desorption of hydrophilic product molecules.

For example, Dai et al. have proposed C<sub>2</sub>H<sub>2</sub> treatment of Pd nanoparticles for enhancement of hydrogenation ability of hydrophobic substrates. The treatment with C<sub>2</sub>H<sub>2</sub> on Pd results in the polymerization of C<sub>2</sub>H<sub>2</sub> into trans-polyacetylene and makes the Pd surface hydrophobic <sup>40</sup>. Such a surface modification helps to accumulate more hydrophobic substrates during catalysis with the enhancement of catalytic activity. As shown in **Figure 10**, the contact angle of water droplets on the Pd surface increased from 32.6° to 64.8° after the C<sub>2</sub>H<sub>2</sub> polymerization, indicating the hydrophobic character of the

Pd surface. Consequently, the modified catalysts exhibited higher activity in the hydrogenation of hydrophobic nitrobenzene but poorer catalytic activity for the hydrogenation of hydrophilic 4-nitrophenol.

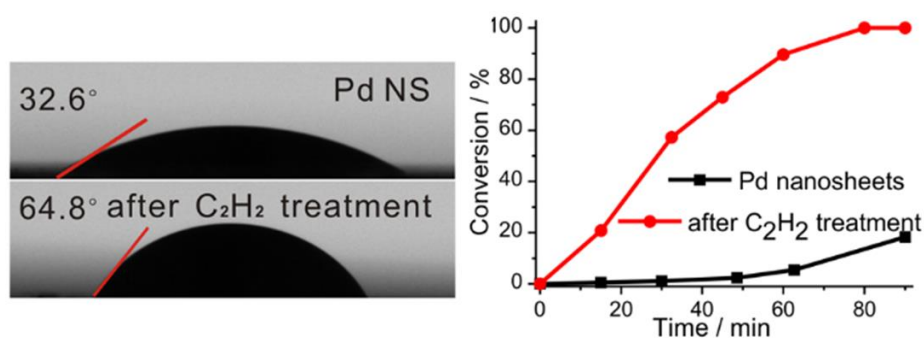


**Figure 10.** Static water contact angle and nitrobenzene hydrogenation catalytic activity over Pd nanosheet before and after C<sub>2</sub>H<sub>2</sub> treatment <sup>40</sup>.

Besides hydrogenation of nitrobenzene, the introduction of surface hydrophilic moieties such as the hydroxyl groups has been demonstrated for promoting the production of hydrogen peroxide (H<sub>2</sub>O<sub>2</sub>) from H<sub>2</sub> and O<sub>2</sub>. H<sub>2</sub>O<sub>2</sub> attracts growing attention as a green stoichiometric oxidant in a wide range of applications. Currently, it is commercially synthesized by the sequential hydrogenation and oxidation of anthraquinones in a mixture of organic solvents. The state-of-the-art technology suffers from high energy input, a significant generation of waste, and complex liquid-liquid separations. The direct synthesis of H<sub>2</sub>O<sub>2</sub> from molecular hydrogen (H<sub>2</sub>) and oxygen (O<sub>2</sub>) is highly desirable but extremely challenging.

Freitas et al. have confirmed that the ligands with H-bonding groups result in significant enhancement of the selectivity to H<sub>2</sub>O<sub>2</sub> over Pd nanoparticles <sup>102</sup>. They screened a wide range of surface-bound ligands with varying functionalities such as polyethylene glycol (PEG), hexadecyltrimethylammonium bromide (CTAB), mercaptosuccinic acid (MSA), oleylamine (OAm), trioctylphosphine (TOP). The highest selectivity had been related to the ligands with the OH functionality in their structure

(Figure 11), which promotes hydrogenation of the OOH intermediate to  $\text{H}_2\text{O}_2$ . In the case of the ligands without OH functionality, the authors observed an increase in the rate of the  $\text{H}_2\text{O}_2$  production that scaled with the bulkiness of the ligands ( $\text{TOP} > \text{OAm} > \text{CTAB}$ ). This suggests a possible effect induced by steric hindrance arising from the ligands. Deep characterization suggested a positive relationship between the rate of  $\text{PdH}_x$  formation and  $\text{H}_2\text{O}_2$  selectivity.

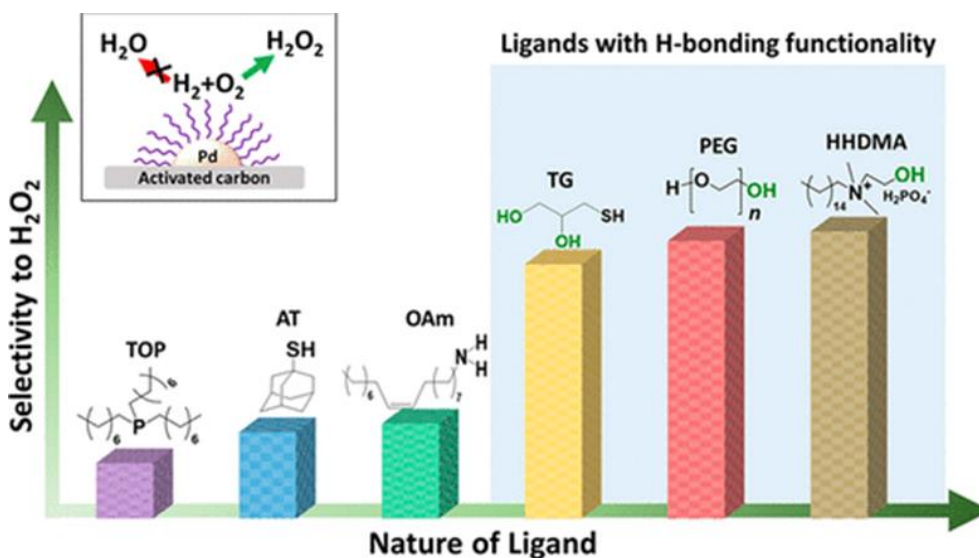


**Figure 11.** Effect of various ligands on the selectivity to  $\text{H}_2\text{O}_2$  over Pd catalyst. The selectivity to  $\text{H}_2\text{O}_2$  enhanced by the ligands with H-bonding functionality<sup>102</sup>.

#### 2.1.4. Molecular orientation

Molecular orientation is related to the changes of the reactant molecule configuration approaching the catalyst surface due to the presence of modifier tails. In comparison with molecular affinity, molecular orientation does not have any specific intermolecular interaction between promoters and reactants but has spatial hindrance. Molecular orientation has been demonstrated during the hydrogenation of cinnamaldehyde. Tuning the structure of the SAM tail facilitated appropriately positioned aromatic stacking interactions between the reactant and the modifier. Cinnamaldehyde is an  $\alpha$ ,  $\beta$ -unsaturated aldehyde of significant industrial importance<sup>143</sup>. Typically, on transition

metal catalysts, the major product is formed via hydrogenation of the double bond to produce hydrocinnamaldehyde. However, the more industrially valuable product is cinnamyl alcohol formed by hydrogenation of the aldehyde. Platinum is one of the most selective metals for producing cinnamyl alcohol<sup>80</sup>. To demonstrate this concept, a variety of SAMs with organic tails were tested to determine their effect on selectivity. The results demonstrate that the selectivity could be increased from ~25% on the uncoated Pt catalysts to over 95% using the catalyst modified with 3-phenylpropanethiol. This modifier provides aromatic stacking interactions between the modifier and reagent for selective conversion of the aldehyde moiety.

The proposed adsorption mechanism for this highly selective system is shown in **Figure 12**. Linear alkane chains with no specific interaction with cinnamaldehyde provide a modest selectivity improvement over uncoated catalysts. This nonspecific effect was induced by the presence of sulfur independently of the alkanethiol tail length. Reducing the distance between the SAM phenyl moiety and the catalyst resulted in a low selectivity to the desired product. Earlier, it has been shown that binding in a horizontal configuration favors olefin hydrogenation, while binding vertically favors the hydrogenation of the aldehyde.

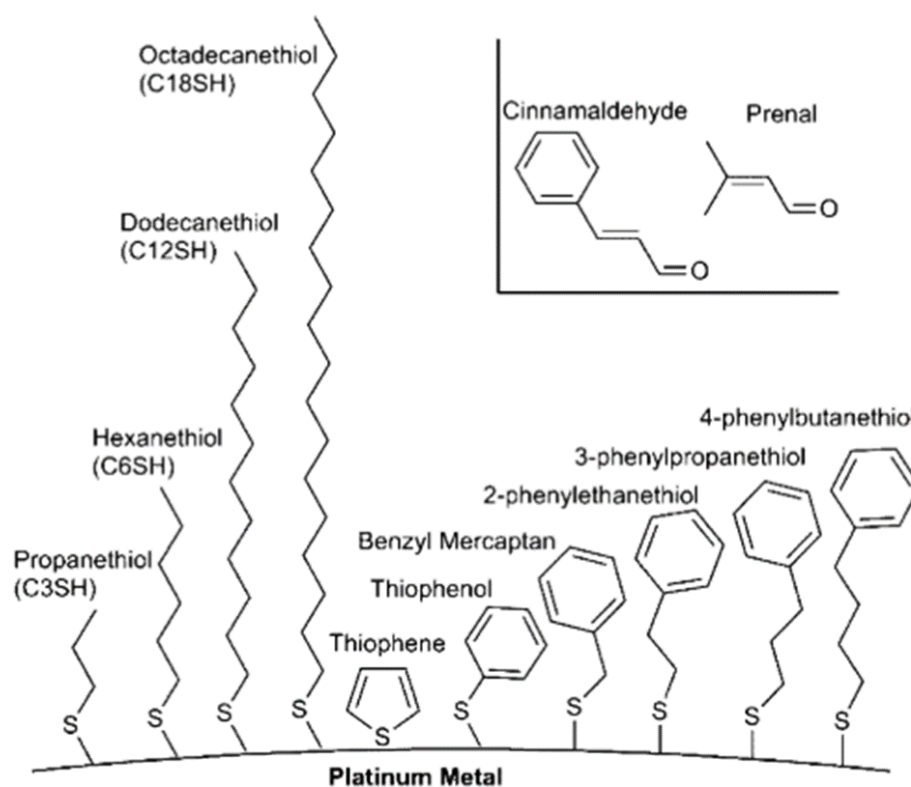


**Figure 12.** Proposed adsorption mechanism depicting the favorable orientation of cinnamaldehyde induced by 3-phenylpropanethiol SAM modifiers <sup>143</sup>.

The spatial hindrance of promoters allowed the penetration of the reactant molecules with a small functional group to the catalytic surface. Thus, molecular orientation favors the reactions happening on the small functional group of the molecules. One example is the hydrogenation of cinnamaldehyde over amines-capped Pt<sub>3</sub>Co nanoparticles <sup>69</sup>. It is well known that hydrogenation of unsaturated aldehydes (CAL) over metal catalysts thermodynamically favors the formation of saturated aldehydes (hydrocinnamaldehyde, HCAL) rather than unsaturated alcohol (hydrocinnamyl alcohol, HCOL). OAm can form an ordered arrangement on the Pt surface and the long carbon chains impart steric hindrance, so that the CAL molecules do not lie flatly on the nanoparticle surface. Computationally, the CAL molecules can only enter into the array of oAm molecules with their aldehyde groups interacting with the Pt<sub>3</sub>Co (100) surface. The C=C bonds are far away from the catalytically active surface (**Figure 13**).



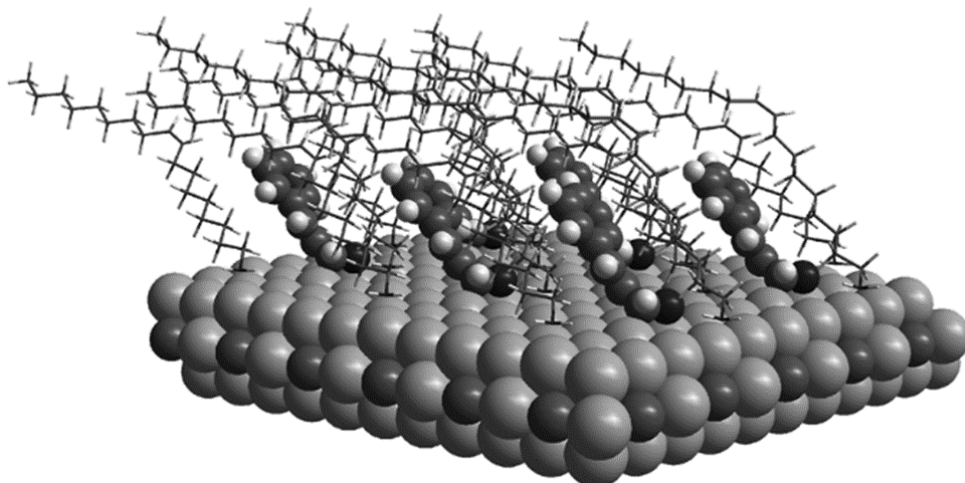


**Figure 13.** Optimized structure of CAS adsorption on the Pt<sub>3</sub>Co (100) surface capped by oAm <sup>69</sup>.

Adjusting the adsorption configuration of oxygen molecules on the Pd surface can promote H<sub>2</sub>O<sub>2</sub> selectivity in direct H<sub>2</sub>O<sub>2</sub> production. For example, Lari et al. have disclosed that the ligand-modified palladium nanoparticles deposited on a carbon carrier efficiently catalyze the direct synthesis of H<sub>2</sub>O<sub>2</sub> <sup>144</sup>. Catalytic testing demonstrated that the selectivity increased with the HHDMA ligand content from 10% for naked nanoparticles up to 80%. As rationalized by DFT calculations, this behavior arises from the adsorption of O<sub>2</sub> and hydroperoxyl radicals. These intermediates are flattened on the Pd (111) surface (**Figures 14**), thus favoring the cleavage of the O-O bond and leading to the water production. In contrast, on Pd (111)-HHDMA, the electrostatic interaction of the adsorbed intermediates with the H<sub>2</sub>PO<sub>4</sub><sup>-</sup> group and quaternary ammonium headgroups of the HHDMA molecule enables the peculiar vertical configuration of the intermediate, impeding the cleavage of the O-O bond and its over-hydrogenation to water, thus increasing the selectivity to H<sub>2</sub>O<sub>2</sub>.



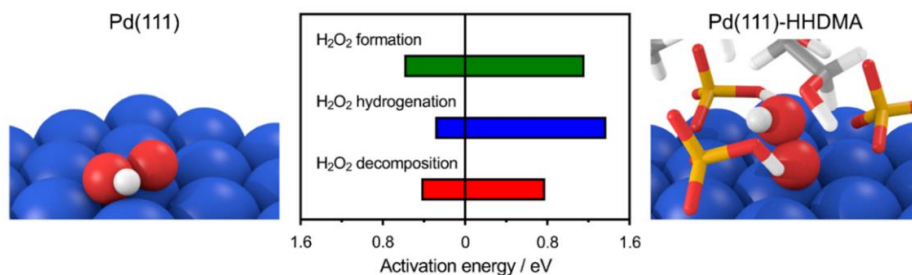


**Figure 14.** Activation energies for the direct synthesis of  $H_2O_2$  and the side reactions leading to water formation by  $H_2O_2$  hydrogenation and decomposition <sup>144</sup>.

### 2.1.5. Surface molecular imprinting

Molecular imprinting is a powerful strategy to create recognition cavities or active sites within heterogeneous catalysts by using a template molecule to control the reactant selectivity <sup>145, 146</sup>. The imprinted catalysts show high selectivity for the transformation of the molecules displaying similar size or shape with the template. The conventional strategy for the preparation of imprinted catalysts involves polymerization of monomers around the template molecules and followed by the template removal.

Recently, surface molecularly imprinted  $TiO_2$  catalyst has been reported by Christian et.al. for the major enhancement of selectivity in photocatalytic oxidations and transfer hydrogenations <sup>136</sup>. The imprinted  $TiO_2$  was prepared by the template-assisted atomic layer deposition (ALD) method. As shown in **Figure 15**, organic template molecules were firstly adsorbed on  $TiO_2$  surface followed by deposition of  $Al_2O_3$  thin layer by ALD, finally, removal of the organic templates by  $O_3$  oxidation leads to the molecular imprinted  $TiO_2$  catalyst with sieved  $Al_2O_3$  layer. As confirmed by photocatalytic oxidation and reduction, the imprinted  $TiO_2$  catalyst with suitable template molecules shows steric hindrance for large reactant molecules in the catalysis.

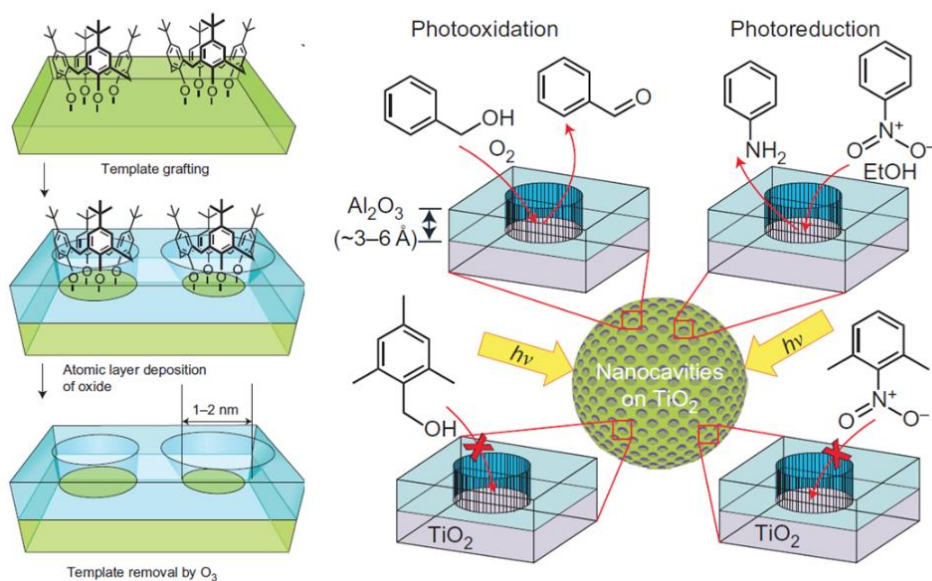


**Figure 15.** Surface molecular imprinting over  $\text{TiO}_2$  with organic template and its steric hindrance in photocatalytic oxidation and reduction <sup>136</sup>.

Besides performing molecular imprinting over  $\text{TiO}_2$  surface, most recently, our group developed the surface molecular imprinting method over the metal surface for size-dependent hydrogenation reactions <sup>147</sup>. Our strategy involves the sequential adsorption over the Pd surface of an aromatic template molecule (e.g., benzene) followed by poisoners (3-Dimethylaminopropylamine, DMAPA) resulting in the formation of non-poisoned active islands with pre-determined shape and size. Because of steric constraints, these active islands exhibit high selectivity in the hydrogenation of the aromatic molecules with the size and shape corresponding to the templates (**Figure 16**). Furthermore, we applied the molecularly imprinted Pd catalyst for selective hydrogenation of benzene from the mixture of aromatics. The elaborated process exhibited excellent catalytic performance and indicated the potential application in selective benzene removal.

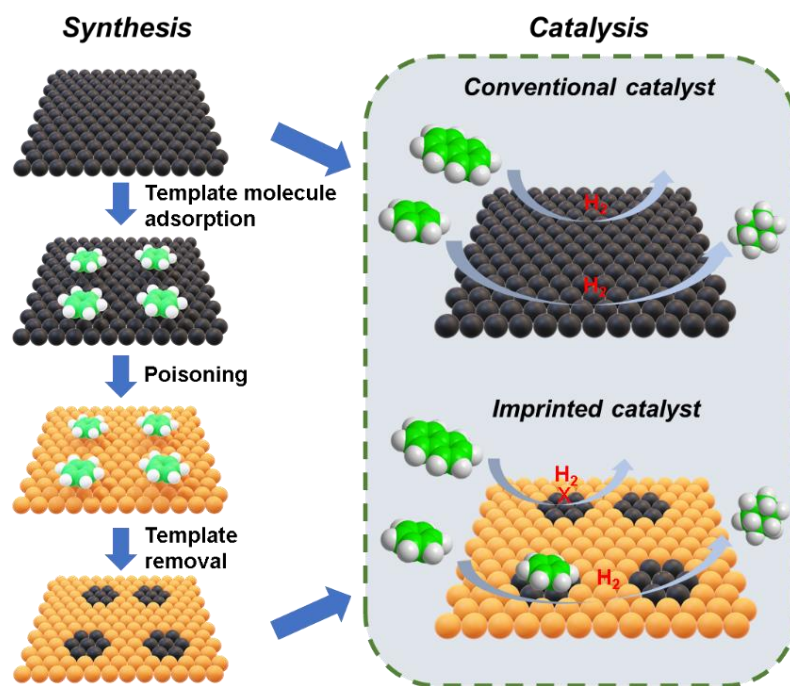


**Figure 16.** Surface molecular imprinting over metal surface for size-dependent hydrogenation reactions <sup>147</sup>.

## 2.2. Electronic effects

The electronic structure and density of active sites in metal catalysts are important for heterogeneous catalysis. The electronic effect is due to the surface metal atoms in the catalysts having different local electronic structures, which interact differently with the reacting molecules. Several theories have been developed to define the relationship between the electronic state of metal and its catalytic activity. For example, a *d*-band center theory was proposed and developed by Norskov et al. for transition metal catalysis <sup>11</sup>. It has been reported that the modification of Pt (111) surface with subsurface 3*d* transition metals changes the *d*-band center of surface Pt. The dissociative adsorption energy of H<sub>2</sub> and O<sub>2</sub> on such Pt (111) surface exhibited a linear trend with the *d*-band center. The more positive is the *d*-band center, the lower is the dissociative adsorption energy of H<sub>2</sub> and O<sub>2</sub>. The description of the electronic effects of non-metallic promoters on the metal surface is still a challenge. Although the electronic effects of ligands have

been widely applied to optimize homogeneous catalysis by metal complexes, it has been much less recognized in the field of heterogeneous catalysis. The interactions between non-metallic promoters and metal atoms are more complex. The electronic effect of the modified metal catalysts is usually interpreted in terms of electron donation and electron withdrawal.

The universal consequence of electron donation and the electron withdrawal effect of promoters is the modification of the electronic density of the surface metals. For example, the electron donation promoters such as N- and P-based elements result in negatively charged active sites. Catalyst modification with electron withdrawal promoters like S- and halogen-based species leads to the positively-charged metal surface. The change of the electronic density of the metal surface consequently alters the catalytic properties. For example, the negatively charged metal surface enhances the adsorption of electron-deficient molecules but suppresses the reaction with electron-rich counterparts. Guo et al. have investigated the effect of the electronic density of Pd nanoparticles on the hydrogenation reactions <sup>73</sup>. As shown in **Figure 17**, the authors deposited Pd nanoparticles on a PPh<sub>3</sub> cross-linked in the FDU-12 support. The electron-donating effect of PPh<sub>3</sub> increased the surface electronic density of Pd NPs as well as the activity in the reactions involving electrophilic substrates.

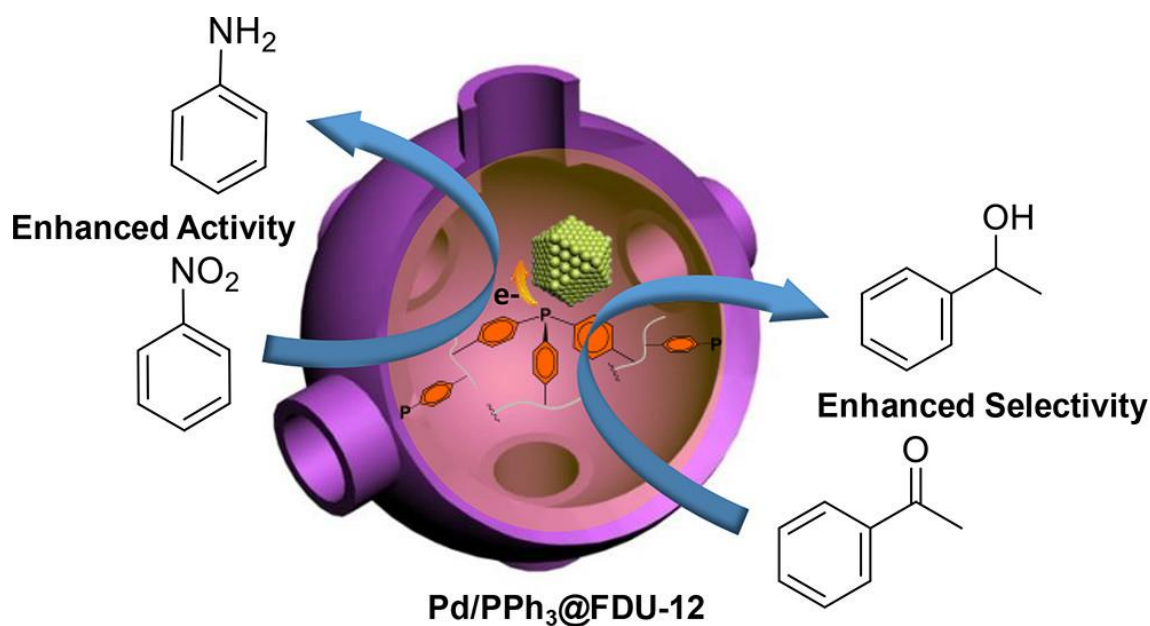


**Figure 17.** Hydrogenation reactions over Pd/PPh<sub>3</sub>@FDU-12 catalyst <sup>73</sup>.

The electronic structure of the metal surface strongly affects the catalytic properties.

**Figure 18** shows a volcano-type curve that relates the intrinsic activity and adsorption energy for different metals. This curve illustrates the Sabatier principle <sup>11</sup>. It states that the interactions between the catalyst and the substrate should be "just right", neither too strong nor too weak. If the interaction is too weak, the substrate will fail to bind to the catalyst and no reaction will take place. On the other hand, if the interaction is too strong, the product fails to desorb. The observed abnormal catalytic results derived from electronic state changes could be often explained as the movement of the modified catalyst on the volcano-type curve.

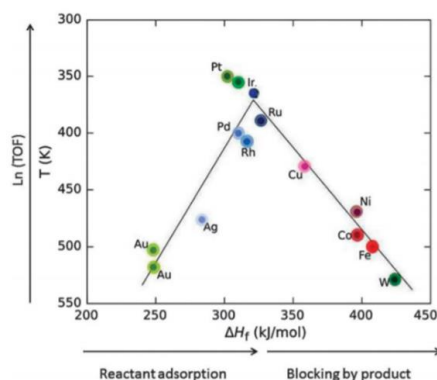
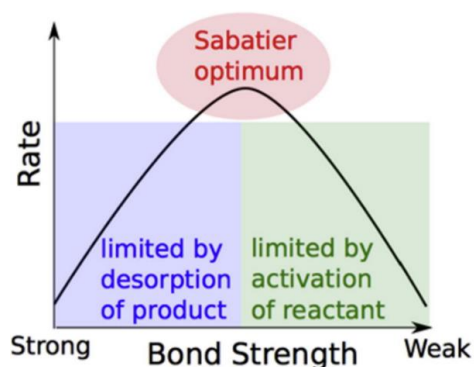


**Figure 18.** Volcano-type relationship between metals and their catalytic activity <sup>11</sup>.

### 2.2.1. *Electronic donation*

The electronic donation effect normally exists in the elements that have a lone pair of electrons. The usually used promoters for electronic donation are N-based, P-based, and carbenes. Polymers with good solubility are widely used as capping agents to control the growth of nanoparticles and protect them from aggregation. The polymers on the metal surface act as promoters during heterogeneous catalysis. For example, PVP has been widely used as a capping agent for the transition metal nanoparticle synthesis. The electronic effects of Au nanoparticles modified by PVP have been studied by Hironori et al.<sup>42</sup>. The electronic density of PVP@Au nanoclusters was investigated by CO-FTIR. It is known that the CO molecules adsorb over clusters of Au atoms. Thus, the stretching frequency of adsorbed CO mainly reflects the electron density on the adsorption sites. The shifts of vibration frequency ( $\nu_{\text{CO}}$ ) towards higher and lower wavenumbers are relative to that of free CO, when CO is adsorbed over positively and negatively charged Au sites, respectively. Larger Au particles are less affected by PVP and the CO adsorption spectra are comparable to that for the bulk gold. However, the CO adsorption peaks over small Au nanoparticles significantly shift to lower frequency from those of large ones. The lower-frequency shift of  $\nu_{\text{CO}}$  on small Au nanoparticles has been assigned to CO adsorbed on negatively charged Au sites.

Sebastiano et al. have reported using diffuse reflectance infrared spectroscopy (DRIFTS) the accessibility and electronic effect of metal sites by monitoring the adsorption of CO as a probe molecule<sup>49</sup>. Pd NPs were synthesized with coating by PVA and deposited on Al<sub>2</sub>O<sub>3</sub> supports by sol immobilization. As shown in **Figure 19**, adsorbed CO on Pd/Al<sub>2</sub>O<sub>3</sub> exhibits three main signals. The signal at 2098 cm<sup>-1</sup> is due to CO linearly bound to the Pd particle corners. The signal at 1980 cm<sup>-1</sup> is related to  $\mu^2$  bridge-bonded CO on the Pd (100) facets, while that at 1945 cm<sup>-1</sup> is attributed to  $\mu^2$  bridge-bonded CO on the Pd (111) planes. After PVA coating, the new peak appears at 1960 cm<sup>-1</sup> and 1925

$\text{cm}^{-1}$ , which were ascribed to the perturbation of the  $\mu^2$  bridge-bonded CO on Pd (100) facets and  $\mu^2$  bridge-bonded CO on Pd (111) planes, respectively. This shift is due to the electron donation effect of PVA on the Pd surface. The back-donation from Pd to the  $\pi^*$  antibonding orbitals of CO lowers the vibrational frequency of adsorbed CO.

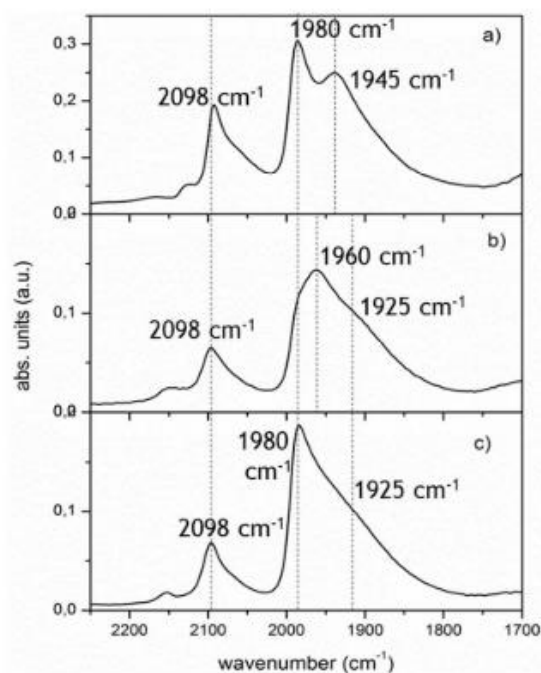


**Figure 19.** DRFTIR spectra of adsorbed CO on (a) 5 wt% Pd/Al<sub>2</sub>O<sub>3</sub>, (b) 5 wt% Pd@PVA/Al<sub>2</sub>O<sub>3</sub> and (c) calcined 5 wt% Pd@PVA/Al<sub>2</sub>O<sub>3</sub><sup>49</sup>.

Chen et al. have reported the preparation of uniform ultrathin ( $\sim 1.1$  nm in diameter) Pt nanowires with ethylenediamine (EDA) chelated on their surfaces (denoted as EDA-Pt NWs). The promoted Pt nanowires were used as model catalysts for the hydrogenation of nitroaromatics<sup>60</sup>. Due to the electron donation from EDA to Pt NWs, the surface of Pt NWs became electron-rich. This interfacial electronic effect makes the Pt NWs favorable for the adsorption of electron-deficient reactants but disfavors the adsorption of electron-rich substances (N-hydroxylanilines). The reaction mechanism has been supported by the DFT calculation. The adsorption free energies ( $\Delta G_{\text{ads}}$ ) of nitrobenzene, nitrosobenzene and N-hydroxylaniline on bare Pt NWs are -1.27, -1.48 and -0.89 eV, respectively. It



indicates that all of these N-containing aromatics are readily adsorbed on the pristine Pt catalysts and undergo hydrogenation. This explains the poor selectivity for N-hydroxylaniline over Pt black. As shown in **Figure 20**,  $\Delta G_{po}$  for nitrobenzene and nitrosobenzene were calculated to be -0.55 and -0.87 eV, respectively, whereas  $\Delta G_{po}$  for N-hydroxylaniline was 0.41 eV. These changes in free energy can be explained in terms of the change in the spatial distribution of the electronic density. In the presence of EDA, *d* orbitals of Pt are nearly fully occupied. This favors the adsorption of electron-deficient substrates through *d*- $\pi^*$  donation but disfavors electron-rich substrates because of the negatively charged Pt surface. Moreover, Pt black was treated with [Pt(EDA)<sub>2</sub>](acac)<sub>2</sub> to allow the deposition of Pt-EDA chelating units on its surface. A series of nitroaromatics with various substitutions (1-fluoro-4-nitrobenzene, 1-chloro-4-nitrobenzene, 1-bromo-4-nitrobenzene, 1-methyl-4-nitrobenzene and 1-methoxy-4-nitrobenzene) have been examined for hydrogenation over the modified Pt black. A significant enhancement of the selectivity towards the N-hydroxylaniline derivatives was observed.

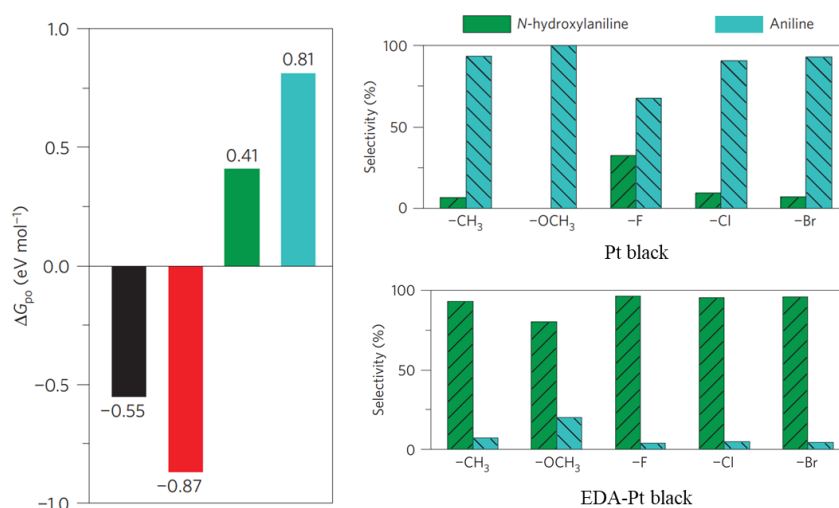


**Figure 20.** Mechanism of catalytic selectivity of EDA-Pt NWs. Left: Free energies ( $\Delta G_{po}$ ) for the adsorption of N-containing aromatics over EDA pre-coated Pt NWs. Black, nitrobenzene; red, nitrosobenzene; green, N-hydroxylaniline; blue, aniline. Right:



*Comparison of the catalytic performances for the hydrogenation of substituted nitrobenzene over the commercial Pt black before and after EDA modification*<sup>60</sup>.

Recently, N-heterocyclic carbenes (NHCs) have been proposed as a class of electronic donation promoters for metal nanocatalysts. NHCs are a unique class of ligands, which is widely applied in the fields of coordination chemistry and homogeneous catalysis. Their electron-rich nature leads to strong bonding to metals. In general, they act as strong  $\sigma$ -donor and weak  $\pi$ -acceptor ligands and are capable to influence the reactivity and selectivity of homogeneous transition metal catalysts. For example, Johannes et al. have investigated the influence of the NHC ligands on the activity of the Pd/Al<sub>2</sub>O<sub>3</sub> catalyst<sup>65</sup>. They choose the hydrogenolysis of bromobenzene as the benchmark reaction to investigate the activating effect of NHCs. The activation of bromobenzene should be facilitated in the presence of electron-donating ligands similar to homogeneous catalysis. A significant accelerating effect of ImesNHCs was observed with aromatic N-substituents being the most effective ligands (IPr, IMes). NHCs bearing alkyl N-substituents (ICy, IMe) were less efficient in the promotion of hydrogenolysis but superior to unmodified Pd/Al<sub>2</sub>O<sub>3</sub>.

### *2.2.2. Electronic withdrawal*

The electronic withdrawal effects relevant to the use of non-metallic promoters for metal catalysts have been less reported. The most-reported promoters for electronic withdrawal are S-based species. For example, Zhao et al. have used the thiol-treated ultrathin Pd nanosheets as a model catalyst for semi-hydrogenation of internal alkynes<sup>101</sup>. The ultrathin structure of Pd NSs makes it feasible to directly visualize the change in the surface structure of Pd NSs upon their reaction with thiols via electron microscopy. They revealed that upon adsorption of 3,4-difluorothiols (HSPhF<sub>2</sub>), C-S bonds in thiols can be broken forming a Pd surface modified with both thiolates and sulfides.

As shown in **Figure 21**, the XPS data confirmed the co-presence of  $S^{2-}$  and thiolate on the thiol-treated Pd NSs. Two main sulfur components at 162.9 and 163.8 eV were assigned to  $S^{2-}$  and  $SR^-$ , respectively. The presence of  $S^{2-}$  proves the S-C bond cleavage in the thiol modification process. Moreover, the binding energy of Pd 3d in distorted Pd NSs displayed a slight shift toward higher binding energy than that of unmodified NSs, indicating that Pd had been partially oxidized. It is worth noting that modification with sulfur will lead to the sulfur atoms entering the first coordination shell around the Pd atoms. The 3D distributions of Pd and S elements were characterized by high-sensitivity low-energy ion scattering spectroscopy (**Figure 21**). Even with the increased depth of analysis enabled by Ar ion sputtering, the presence of sulfur species was still revealed, indicating the incorporation of  $S^{2-}$  into the inner lattice of Pd.

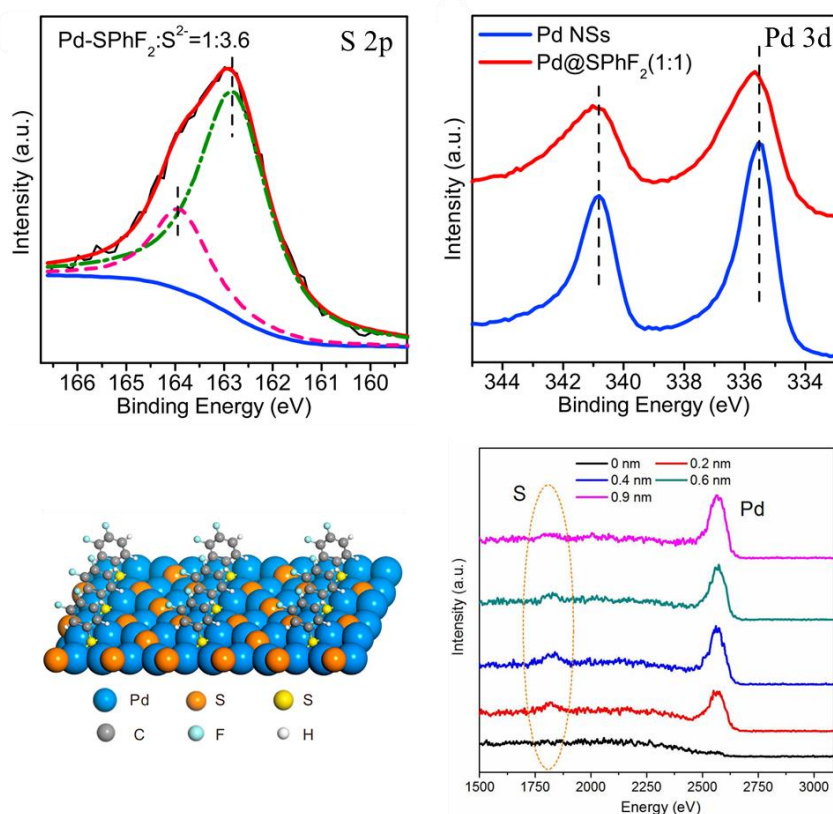


**Figure 21.** Structure analysis of the Pd@SPhF<sub>2</sub> (1:1) catalyst. Top: High-resolution XPS spectra of the S 2p region and the Pd 3d region; Bottom: The LEISS spectra for with different detected depths <sup>101</sup>.

### 2.3. Bifunctionality

Design of efficient chemical processes requires integration of multiple catalytic steps in a one-pot catalytic system<sup>148-151</sup>. Besides modulation of the activity and selectivity of metal sites, the presence of the non-metallic promoters can create bifunctional active sites like metal-acid or metal-basic sites. The introduction of bifunctionality on metal catalysts by surface modification is an alternative way for the design of a single heterogeneous catalyst for multiple-step or cascade reactions (e.g. hydrogenation and deoxygenation, acetalization and hydrogenolysis). Bifunctionality of heterogeneous metal catalysts takes the advantage of both homogeneous and heterogeneous catalysts affording simultaneous high activity and easy separation. Moreover, in comparison with the conventional bifunctional catalysts (e.g., deposition of metal nanoparticles on acidic or basic supports), modification by non-metallic promoters provides tunability of the strength and spatial location of bifunctional sites. Depending on the nature of promoters, the bifunctional sites could be introduced on the surface of the support or metal nanoparticles or on both entities. Different position of promoters leads to different distances between metal and acid/base sites, which is of significant importance in catalysis. While the location of acid/base sites on the metal surface creates intimate bifunctional sites, the deposition of promoters on the supports leads to spatially separated metal-acid (or metal-base) sites.

#### 2.3.1. Spatially separated bifunctional sites

Several papers have reported the construction of spatially separated bifunctionality over heterogeneous catalysts by modifications of the support surface. For example, Zhang et al. have reported modification of the Pt/Al<sub>2</sub>O<sub>3</sub> catalysts with organic phosphonic acids by grafting phosphonate ligands on the Al<sub>2</sub>O<sub>3</sub> support<sup>29</sup>. As shown in **Figure 22**, 5 wt% Pt/Al<sub>2</sub>O<sub>3</sub> catalyst modified by methyl phosphonic acid (MPA) was characterized by

STEM-EDS, XPS, and FTIR. The deposition of MPA on  $\text{Al}_2\text{O}_3$  was demonstrated by STEM-EDS. The EDS peak deconvolution demonstrated negligible phosphorus content on the platinum nanoparticles. Deposition of MPA on platinum black showed minimal phosphorus signal (phosphorus  $2p$ ) according to XPS analysis, whereas MPA/5%Pt/ $\text{Al}_2\text{O}_3$  showed significant phosphorus coverage. Also, the MPA deposition on 5%Pt/ $\text{Al}_2\text{O}_3$  does not alter the platinum  $4d$  binding energy, further confirming the absence of MPA on platinum. The FTIR spectra showed the appearance of C-H stretching vibration peaks after the MPA deposition on 5%Pt/ $\text{Al}_2\text{O}_3$ . Moreover, phosphonic acid deposition was found to introduce Brønsted acid sites to the catalyst. A characteristic pyridinium ion peak around  $1540\text{ cm}^{-1}$  was observed in the diffuse reflectance infrared Fourier transform spectra (DRIFTS) after pyridine adsorption. The introduced Brønsted acidity suggests retention of P-OH groups, when phosphonic acids were bound on the  $\text{Al}_2\text{O}_3$  support. Overall, the characterization results showed that: (1) phosphonic acid was bounded selectively to  $\text{Al}_2\text{O}_3$  rather than platinum, (2) modification with phosphonic acid introduced Brønsted acid sites and (3) phosphonic acid retained their organic functionality and did not restructure  $\text{Al}_2\text{O}_3$ .

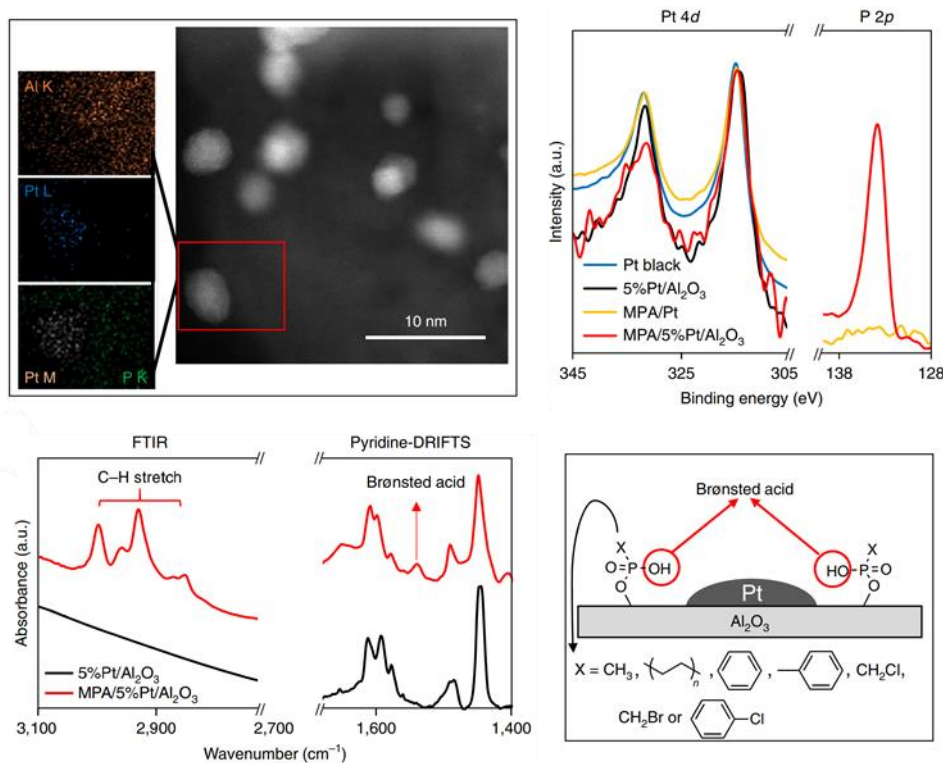


**Figure 22.** Phosphoric acid modified  $Pt/Al_2O_3$  catalysts. Top: STEM-EDS elemental mapping and XPS analysis; Bottom: FTIR and pyridine DRIFTS spectra <sup>29</sup>.

Construction of spatial separated basic sites around metal nanoparticles was achieved by Liu et al <sup>152, 153</sup>. They reported a Schiff base modified Au catalyst for catalytic decomposition of formic acid to hydrogen. The Au@Schiff-SiO<sub>2</sub> catalyst was prepared by one-pot aldime condensation (formaldehyde and 3-aminopropyl-triethoxysilane) and in situ reduction of gold precursor (**Figure 23**). Schiff base on the Au@Schiff-SiO<sub>2</sub> catalyst facilitates the O-H bond dissociation of FA to produce CH<sub>2</sub>=NH<sup>+</sup>- species. Such protonated Schiff base promotes the β-hydride elimination in the gold-formate complex to produce CO<sub>2</sub> and H<sub>2</sub>. Thus, the cooperation of Au and Schiff base at the interface of the catalyst leads to efficient H<sub>2</sub> production from formic acid (**Figure 23**).

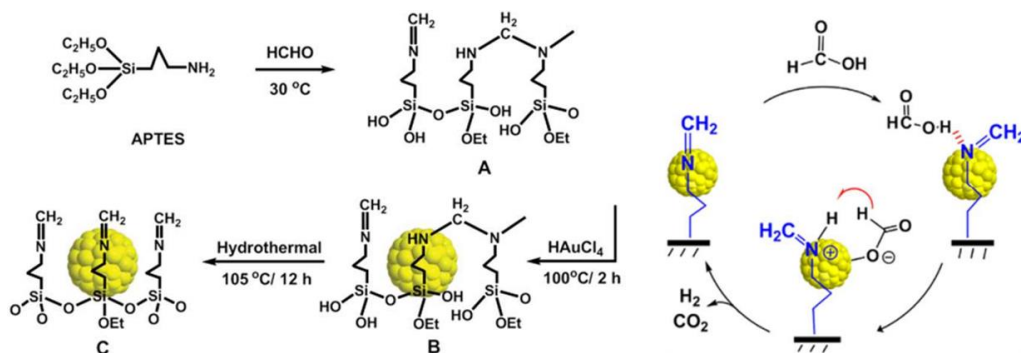


**Figure 3.** Schiff base modified Au catalysts. Left: preparation procedures; Right: Proposed reaction mechanism for the dehydrogenation of formic acid <sup>153</sup>.

### 2.3.2. Intimate bifunctional sites

In comparison with spatial separated bifunctional sites, intimate bifunctional sites could have synergy and catalyze the conversion of a reactant molecule simultaneously <sup>151, 154</sup>. Different from modification of support, intimate bifunctional sites could be generated by the modification of metal surface. These intimate bifunctional sites feature a high synergic effect in catalysis in comparison with spatially separated counterparts.

Integration of both metallic active sites and acid sites is of significant importance in numerous important reactions, especially for the conversion of biomass-derived platforms. While metallic active sites exhibit high activity for small molecules activation such as H<sub>2</sub> and O<sub>2</sub>, acid sites facilitate dehydration, cracking, and esterification. For example, hydrodeoxygenation is one of the important examples for the valorization of biomass resources which need both metallic and acid sites for high efficiency.

Recently, our group has modified the Pd catalyst by organic iodides and bromides and disclosed the in-situ generation of Brønsted acidity on the Pd surface under H<sub>2</sub> atmosphere <sup>106, 108</sup>. Notably, the modification was performed by treatment of supported Pd catalyst with organic iodides and bromides in the presence of hydrogen, and the hydrogenolysis of carbon-halogen on the Pd surface led to the selective deposition of I and Br atoms on the Pd surface not on the support. The formed Pd-I and Pd-Br catalysts

were subjected to Pyridine-FTIR to confirm the generation of Brønsted acid sites in the presence of H<sub>2</sub>. Both additions of pyridine or pyridine and H<sub>2</sub> over the initial Pd/Al<sub>2</sub>O<sub>3</sub> catalyst led to a set of typical peaks attributed to pyridine adsorption on the Lewis acid sites the Al<sub>2</sub>O<sub>3</sub> support (**Figure 24**). However, in the co-presence of pyridine and H<sub>2</sub>, the Pd-I catalyst exhibited a new peak at 1540 cm<sup>-1</sup> ascribed to Brønsted acidity. The presence of Brønsted acidity is associated to the partial pressure of H<sub>2</sub>, after the removal of H<sub>2</sub> from the FTIR cell, the Brønsted acidity disappeared and reappeared after the re-addition of H<sub>2</sub>. The generation of Brønsted acidity is corresponding to the H<sub>2</sub> pressure, suggesting the heterolytic dissociation of H<sub>2</sub> over the Pd surface with the formation of Pd (H<sup>-</sup>)-I (H<sup>+</sup>). In this case, the metallic Pd sites and Brønsted acid sites are in the spatial proximity, which could catalyze hydrodeoxygenation and reductive etherification reactions with high efficiency.

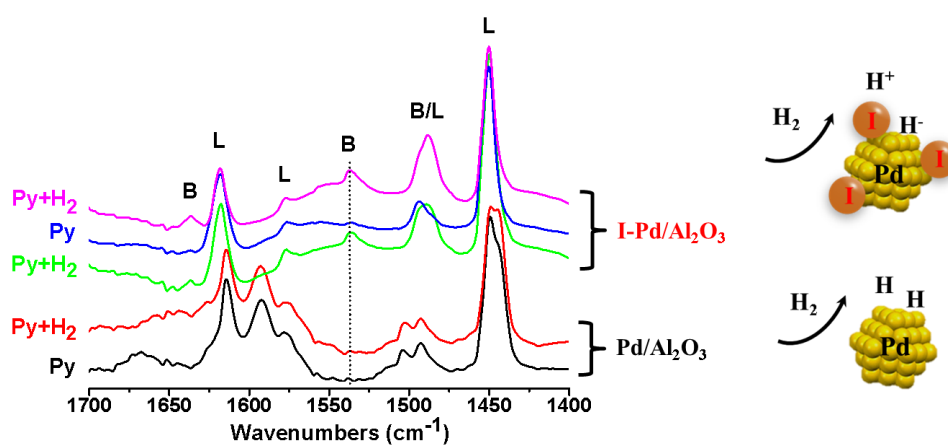


**Figure 24.** *In-situ Brønsted acidity generation over Pd-I catalyst. Left: pyridine-FTIR analysis of Pd/Al<sub>2</sub>O<sub>3</sub> and I-Pd/Al<sub>2</sub>O<sub>3</sub> catalyst; Right: Illustration of heterolytic dissociation of H<sub>2</sub> over Pd/Al<sub>2</sub>O<sub>3</sub> and I-Pd/Al<sub>2</sub>O<sub>3</sub> catalyst <sup>108</sup>.*

The mechanistic studies including hydrogenation of model compounds and activation energy calculation, demonstrated the extremely high deoxygenation ability of the Pd-Br catalyst. Conventional bifunctional catalysts such as metal-zeolite or metal oxide composites contain metal sites over metal nanoparticles and acid sites over the

zeolite or oxide support. The metal and acid sites in these catalysts are often sterically separated and suffer from insufficient intimacy. Different from conventional metal-acid bifunctional catalysts, the Pd-Br systems have both metal and acid sites located on the surface of the same metal nanoparticles. Thus, the activation of the OH groups by acid sites and hydrogenolysis of the C-O bond by metal sites could take place at the same time, leading to a significant decrease in the activation energy of benzyl alcohol hydrodeoxygenation over the Pd-Br catalyst (**Figure 25**).

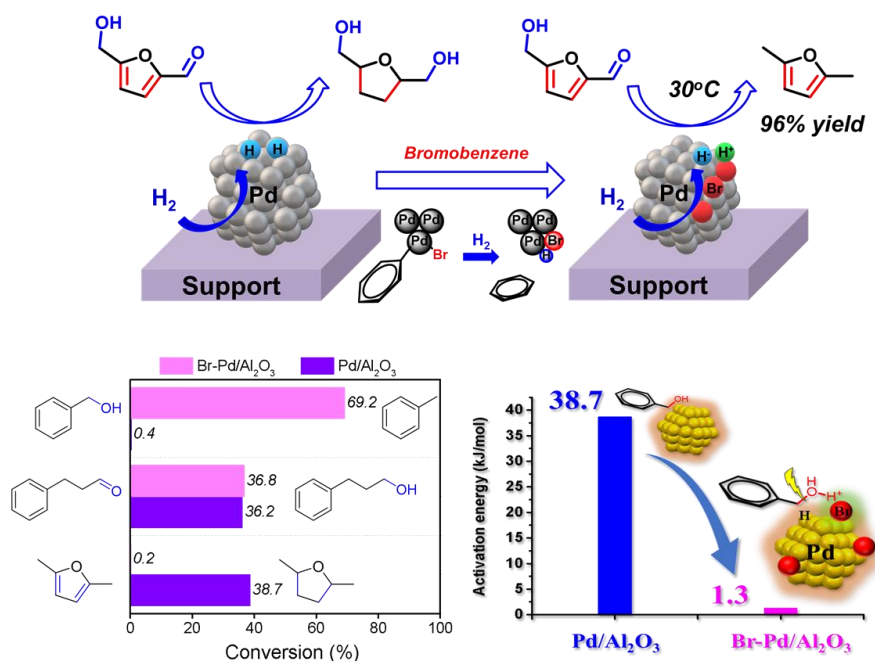


**Figure 25.** Dual Metal-Acid Pd-Br Catalyst. Top: Illustration of hydrodeoxygenation of HMF to DMF over Pd-Br catalyst; Left-bottom: Model reactions over Br-Pd/Al<sub>2</sub>O<sub>3</sub> and Pd/Al<sub>2</sub>O<sub>3</sub> catalyst; Right-bottom: Activation energy of benzyl alcohol hydrogenation over Pd/Al<sub>2</sub>O<sub>3</sub> and Br-Pd/Al<sub>2</sub>O<sub>3</sub><sup>106</sup>.

### 3. Conclusion and perspective

To conclude, this review summarizes the recent progress related to surface modification of metal catalyst by non-metallic elements for a major enhancement of catalytic performance. We discussed steric, electronic effects and bifunctionality



introduced by non-metallic promoters and presented their applications in cascade reactions, e.g. hydrodeoxygenation. However, the surface coordination chemistry of metal nanoparticles is complex, especially in the presence of non-metallic promoters. Intentional design of selective catalysts by surface modification is still a challenge due to the lack of deep understanding of surface chemistry over the metal nanoparticles. Several challenges limit further application of this strategy in real industrial processes.

- (1) Construction of smart catalytic surfaces affording simultaneous high activity and selectivity is still challenging. Normally, the steric effect increases the selectivity but lowers the activity. The electronic effect mostly increases the activity. Bifunctionality increases both activity and selectivity. Thus, the synergy of several effects in one catalytic system makes it possible high activity and selectivity.
- (2) The stability of the non-metallic promoters on the catalyst surface is an important issue for real application. Leaching of promoters in the catalysis will cause loss of the catalytic performance and pollute the products. The development of robust modified catalysts is important and requires more attention. Notably, the stability depends only on the promoters and metals but also on the operating conditions such as temperature, solvent, external pressure and so on. In some cases, a modifier can highly efficient for achieving excellent performance, however, it is not stable and its leaching during catalysis is inevitable. Continuous feeding of promoters into the catalytic systems can be a solution. However, it can affect the cost of the final product, which will require further purification.
- (3) The understanding of the promotion effect relies on deep characterizations of the materials. For example, XAS would be a powerful tool to identify the coordination chemistry and electronic state of metal nanoparticles imposed by the promoters.

Also, modeling can offer great help for the understanding of the multiple interactions between promoters and catalyst surface, reactants and catalyst surface, as well as promoters and reactants.

- (4) Kinetic studies are useful to determine the roles of promoters in catalysis. The influence of promoters could be better ascribed to steric or electronic effects by the changes of apparent activation energy and intrinsic activity of surface sites often expressed as Turnover Frequency (TOF). While the steric effect changes the numbers of active sites, the electronic and bifunctional effects alter the intrinsic properties of active sites. Thus, the changes of activation energy are normally accompanied by the changes of intrinsic activity of surface sites, which could be imposed by electronic effect or bifunctionality or by both phenomena. It is worth noting that the same specific promoter can work differently in different reactions. Another point regarding reactions is the development of intimate bifunctionality on the supported metal catalyst. The bifunctional catalyst prepared by surface modifications integrates both advantages of homogeneous and heterogeneous catalysis, that is high activity and catalyst stability, which could have further applications in the industrial important reactions such as isomerization, biomass conversions and CO<sub>2</sub> conversions.

## Acknowledgments

The authors thank Solvay and University of Lille for stipend for the PhD research of D.W. and financial support of this work.

## Declaration of interest statement

The authors declare no competing interests.

## Reference

1. Li, Z.; Ji, S.; Liu, Y.; Cao, X.; Tian, S.; Chen, Y.; Niu, Z.; Li, Y., Well-Defined Materials for Heterogeneous Catalysis: From Nanoparticles to Isolated Single-Atom Sites. *Chem. Rev.*, **2020**, *120* (2), 623-682. DOI: 10.1021/acs.chemrev.9b00311.
2. Liu, L.; Corma, A., Metal Catalysts for Heterogeneous Catalysis: From Single Atoms to Nanoclusters and Nanoparticles. *Chem. Rev.*, **2018**, *118* (10), 4981-5079. DOI: 10.1021/acs.chemrev.7b00776.
3. Zhang, L.; Zhou, M.; Wang, A.; Zhang, T., Selective Hydrogenation over Supported Metal Catalysts: From Nanoparticles to Single Atoms. *Chem. Rev.*, **2020**, *120* (2), 683-733. DOI: 10.1021/acs.chemrev.9b00230.
4. Wang, L.; Chen, W.; Zhang, D.; Du, Y.; Amal, R.; Qiao, S.; Wu, J.; Yin, Z., Surface strategies for catalytic CO<sub>2</sub> reduction: from two-dimensional materials to nanoclusters to single atoms. *Chem. Soc. Rev.*, **2019**, *48* (21), 5310-5349. DOI: 10.1039/c9cs00163h.
5. Zhong, J.; Yang, X.; Wu, Z.; Liang, B.; Huang, Y.; Zhang, T., State of the art and perspectives in heterogeneous catalysis of CO<sub>2</sub> hydrogenation to methanol. *Chem. Soc. Rev.*, **2020**, *49* (5), 1385-1413. DOI: 10.1039/c9cs00614a.
6. Mäki-Arvela, P.; Simakova, I. L.; Murzin, D. Y., One-pot amination of aldehydes and ketones over heterogeneous catalysts for production of secondary amines. *Catal. Rev. Sci. Eng.*, **2021**, 1-68. DOI: 10.1080/01614940.2021.1942689
7. Lu, L.; Zou, S.; Fang, B., The Critical Impacts of Ligands on Heterogeneous Nanocatalysis: A Review. *ACS Catal.*, **2021**, *11* (10), 6020-6058. DOI: 10.1021/acscatal.1c00903.
8. Gu, B.; Peron, D. V.; Barrios, A. J.; Bahri, M.; Ersen, O.; Vorokhta, M.; Smid, B.; Banerjee, D.; Virginie, M.; Marceau, E.; Wojcieszak, R.; Ordonsky, V. V.; Khodakov, A. Y., Mobility and versatility of the liquid bismuth promoter in the working iron catalysts for light olefin synthesis from syngas. *Chem. Sci.*, **2020**, *11* (24), 6167-6182. DOI: 10.1039/d0sc01600d.
9. Owen, J., Nanocrystal structure. The coordination chemistry of nanocrystal surfaces. *Science*, **2015**, *347* (6222), 615-616. DOI: 10.1126/science.1259924.
10. Kano, S.; Tada, T.; Majima, Y., Nanoparticle characterization based on STM and STS. *Chem. Soc. Rev.*, **2015**, *44* (4), 970-987. DOI: 10.1039/c4cs00204k.
11. Norskov, J. K.; Bligaard, T.; Hvolbaek, B.; Abild-Pedersen, F.; Chorkendorff, I.; Christensen, C. H., The nature of the active site in heterogeneous metal catalysis. *Chem. Soc. Rev.*, **2008**, *37* (10), 2163-2171. DOI: 10.1039/b800260f.
12. Liang, G.; Zhou, Y.; Zhao, J.; Khodakov, A. Y.; Ordonsky, V. V., Structure-Sensitive and Insensitive Reactions in Alcohol Amination over Unsupported Ru Nanoparticles. *ACS Catal.*, **2018**, *8* (12), 11226-11234. DOI: 10.1021/acscatal.8b02866.

13. Wu, B.; Zheng, N., Surface and interface control of noble metal nanocrystals for catalytic and electrocatalytic applications. *Nano Today* **2013**, *8* (2), 168-197. DOI: 10.1016/j.nantod.2013.02.006.
14. Liu, P.; Qin, R.; Fu, G.; Zheng, N., Surface Coordination Chemistry of Metal Nanomaterials. *J. Am. Chem. Soc.*, **2017**, *139* (6), 2122-2131. DOI: 10.1021/jacs.6b10978.
15. Nguyen, L.; Tao, F. F.; Tang, Y.; Dou, J.; Bao, X. J., Understanding Catalyst Surfaces during Catalysis through Near Ambient Pressure X-ray Photoelectron Spectroscopy. *Chem. Rev.*, **2019**, *119* (12), 6822-6905. DOI: 10.1021/acs.chemrev.8b00114.
16. Li, C. F.; Zhao, J. W.; Xie, L. J.; Wu, J. Q.; Ren, Q.; Wang, Y.; Li, G. R., Carboxylate Ligands-Promoted Superior Electrocatalytic Performance for Oxygen Evolution Reaction and Their Mechanisms. *Angew. Chem. Int. Ed.*, **2021**, *60* (33), 18129-18137. DOI: 10.1002/anie.202104148.
17. Gavia, D. J.; Shon, Y. S., Catalytic Properties of Unsupported Palladium Nanoparticle Surfaces Capped with Small Organic Ligands. *ChemCatChem*, **2015**, *7* (6), 892-900. DOI: 10.1002/cctc.201402865.
18. Samantaray, M. K.; D'Elia, V.; Pump, E.; Falivene, L.; Harb, M.; Ould Chikh, S.; Cavallo, L.; Basset, J. M., The Comparison between Single Atom Catalysis and Surface Organometallic Catalysis. *Chem. Rev.*, **2020**, *120* (2), 734-813. DOI: 10.1021/acs.chemrev.9b00238.
19. Niu, Z.; Li, Y., Removal and Utilization of Capping Agents in Nanocatalysis. *Chem. Mater.*, **2013**, *26* (1), 72-83. DOI: 10.1021/cm4022479.
20. Rossi, L. M.; Fiorio, J. L.; Garcia, M. A. S.; Ferraz, C. P., The role and fate of capping ligands in colloiddally prepared metal nanoparticle catalysts. *Dalton Trans.*, **2018**, *47* (17), 5889-5915. DOI: 10.1039/c7dt04728b.
21. Wu, W.; Shevchenko, E. V., The surface science of nanoparticles for catalysis: electronic and steric effects of organic ligands. *J. Nanopart. Res.*, **2018**, *20* (9), 255. DOI: 10.1007/s11051-018-4319-y.
22. Zhang, C.; Wang, F., Catalytic Lignin Depolymerization to Aromatic Chemicals. *Acc. Chem. Res.*, **2020**, *53* (2), 470-484. DOI: 10.1021/acs.accounts.9b00573.
23. Chen, S.; Wojcieszak, R.; Dumeignil, F.; Marceau, E.; Royer, S., How Catalysts and Experimental Conditions Determine the Selective Hydroconversion of Furfural and 5-Hydroxymethylfurfural. *Chem. Rev.*, **2018**, *118* (22), 11023-11117. DOI: 10.1021/acs.chemrev.8b00134.
24. Xu, C.; Paone, E.; Rodriguez-Padron, D.; Luque, R.; Mauriello, F., Recent catalytic routes for the preparation and the upgrading of biomass derived furfural and 5-hydroxymethylfurfural. *Chem. Soc. Rev.*, **2020**, *49* (13), 4273-4306. DOI:10.1039/d0cs00041h.
25. van Scodeller, I.; De Oliveira Vigier, K.; Muller, E.; Ma, C.; Guegan, F.; Wischert, R.; Jerome, F., A Combined Experimental-Theoretical Study on Diels-Alder Reaction with Bio-Based Furfural: Towards Renewable Aromatics. *ChemSusChem* **2021**, *14* (1), 313-323. DOI: 10.1002/cssc.202002111.
26. Jiang, S.; Muller, E.; Jérôme, F.; Pera-Titus, M.; De Oliveira Vigier, K., Conversion of furfural to tetrahydrofuran-derived secondary amines under mild conditions. *Green Chem.*, **2020**, *22* (6), 1832-1836. DOI: 10.1039/d0gc00119h.
27. Sergeev, A. G.; Webb, J. D.; Hartwig, J. F., A heterogeneous nickel catalyst for the hydrogenolysis of aryl ethers without arene hydrogenation. *J. Am. Chem. Soc.*, **2012**, *134* (50), 20226-20229. DOI: 10.1021/ja3085912.
28. Liu, Y.; Zhao, G.; Wang, D.; Li, Y., Heterogeneous catalysis for green chemistry based on nanocrystals. *Natl. Sci. Rev.*, **2015**, *2* (2), 150-166. DOI: 10.1093/nsr/nwv014.

29. Zhang, J.; Ellis, L. D.; Wang, B.; Dzara, M. J.; Sievers, C.; Pylypenko, S.; Nikolla, E.; Medlin, J. W., Control of interfacial acid–metal catalysis with organic monolayers. *Nat. Catal.*, **2018**, *1* (2), 148-155. DOI: 10.1038/s41929-017-0019-8.
30. Questell-Santiago, Y. M.; Galkin, M. V.; Barta, K.; Luterbacher, J. S., Stabilization strategies in biomass depolymerization using chemical functionalization. *Nat. Rev. Chem.*, **2020**, *4* (6), 311-330. DOI: 10.1038/s41570-020-0187-y.
31. Sergeev, A. G.; Hartwig, J. F., Selective, nickel-catalyzed hydrogenolysis of aryl ethers. *Science*, **2011**, *332* (6028), 439-443. DOI: 10.1126/science.1200437.
32. Zhang, F.; Zeng, M.; Yappert, R. D.; Sun, J.; Lee, Y. H.; LaPointe, A. M.; Peters, B.; Abu-Omar, M. M.; Scott, S. L., Polyethylene upcycling to long-chain alkylaromatics by tandem hydrogenolysis/aromatization. *Science*, **2020**, *370* (6515), 437-441. DOI: 10.1126/science.abc5441.
33. Du, Y.; Sheng, H.; Astruc, D.; Zhu, M., Atomically Precise Noble Metal Nanoclusters as Efficient Catalysts: A Bridge between Structure and Properties. *Chem. Rev.*, **2020**, *120* (2), 526-622. DOI: 10.1021/acs.chemrev.8b00726.
34. Xie, C.; Yan, D.; Li, H.; Du, S.; Chen, W.; Wang, Y.; Zou, Y.; Chen, R.; Wang, S., Defect Chemistry in Heterogeneous Catalysis: Recognition, Understanding, and Utilization. *ACS Catal.*, **2020**, *10* (19), 11082-11098. DOI: 10.1021/acscatal.0c03034.
35. Schlogl, R., Heterogeneous catalysis. *Angew. Chem. Int. Ed.*, **2015**, *54* (11), 3465-3520. DOI: 10.1002/anie.201410738.
36. Medlin, J. W.; Montemore, M. M., Heterogeneous catalysis: Scaling the rough heights. *Nat. Chem.*, **2015**, *7* (5), 378-380. DOI:10.1038/nchem.2245.
37. Calle-Vallejo, F.; Loffreda, D.; Koper, M. T.; Sautet, P., Introducing structural sensitivity into adsorption-energy scaling relations by means of coordination numbers. *Nat. Chem.*, **2015**, *7* (5), 403-410. DOI: 10.1038/nchem.2226.
38. Jin, R.; Li, G.; Sharma, S.; Li, Y.; Du, X., Toward Active-Site Tailoring in Heterogeneous Catalysis by Atomically Precise Metal Nanoclusters with Crystallographic Structures. *Chem. Rev.*, **2021**, *121* (2), 567-648. DOI: 10.1021/acs.chemrev.0c00495.
39. Zhang, F.; Fang, J.; Huang, L.; Sun, W.; Lin, Z.; Shi, Z.; Kang, X.; Chen, S., Alkyne-Functionalized Ruthenium Nanoparticles: Impact of Metal–Ligand Interfacial Bonding Interactions on the Selective Hydrogenation of Styrene. *ACS Catal.*, **2018**, *9* (1), 98-104. DOI: 10.1021/acscatal.8b04028.
40. Dai, Y.; Liu, S.; Zheng, N., C<sub>2</sub>H<sub>2</sub> treatment as a facile method to boost the catalysis of Pd nanoparticulate catalysts. *J. Am. Chem. Soc.*, **2014**, *136* (15), 5583-5586. DOI: 10.1021/ja501530n.
41. Niu, F.; Xie, S.; Bahri, M.; Ersen, O.; Yan, Z.; Kusema, B. T.; Pera-Titus, M.; Khodakov, A. Y.; Ordonsky, V. V., Catalyst Deactivation for Enhancement of Selectivity in Alcohols Amination to Primary Amines. *ACS Catal.*, **2019**, *9* (7), 5986-5997. DOI: 10.1021/acscatal.9b00864.
42. Tsunoyama, H.; Ichikuni, N.; Sakurai, H.; Tsukuda, T., Effect of electronic structures of Au clusters stabilized by poly(N-vinyl-2-pyrrolidone) on aerobic oxidation catalysis. *J. Am. Chem. Soc.*, **2009**, *131* (20), 7086-7093. DOI: 10.1021/ja810045y.
43. Chen, K.; Wu, H.; Hua, Q.; Chang, S.; Huang, W., Enhancing catalytic selectivity of supported metal nanoparticles with capping ligands. *Phys. Chem. Chem. Phys.*, **2013**, *15* (7), 2273-2277. DOI: 10.1039/c2cp44571a.
44. Freakley, S. J.; Agarwal, N.; McVicker, R. U.; Althahban, S.; Lewis, R. J.; Morgan, D. J.; Dimitratos, N.; Kiely, C. J.; Hutchings, G. J., Gold–palladium colloids as catalysts for hydrogen peroxide synthesis, degradation and methane oxidation: effect of the PVP stabiliser. *Catal. Sci. Technol.*, **2020**, *10* (17), 5935-5944. DOI: 10.1039/d0cy00915f.

45. Yang, Y.; Liu, H.; Li, S.; Chen, C.; Wu, T.; Mei, Q.; Wang, Y.; Chen, B.; Liu, H.; Han, B., Hydrogenolysis of 5-Hydroxymethylfurfural to 2,5-Dimethylfuran under Mild Conditions without Any Additive. *ACS Sustain. Chem. Eng.*, **2019**, *7* (6), 5711-5716. DOI: 10.1021/acssuschemeng.8b04937.
46. Zhao, J. P.; Hernández, W. Y.; Zhou, W. J.; Yang, Y.; Vovk, E. I.; Wu, M.; Naghavi, N.; Capron, M.; Ordonsky, V., Nanocell type Ru@quinone core-shell catalyst for selective oxidation of alcohols to carbonyl compounds. *Appl. Catal. A-Gen.*, **2020**, *602*, 117693. DOI: 10.1016/j.apcata.2020.117693.
47. Jones, S.; Qu, J.; Tedsree, K.; Gong, X. Q.; Tsang, S. C., Prominent electronic and geometric modifications of palladium nanoparticles by polymer stabilizers for hydrogen production under ambient conditions. *Angew. Chem. Int. Ed.*, **2012**, *51* (45), 11275-11278. DOI: 10.1002/anie.201206035.
48. Shifrina, Z. B.; Matveeva, V. G.; Bronstein, L. M., Role of Polymer Structures in Catalysis by Transition Metal and Metal Oxide Nanoparticle Composites. *Chem. Rev.*, **2020**, *120* (2), 1350-1396. DOI: 10.1021/acs.chemrev.9b00137.
49. Campisi, S.; Ferri, D.; Villa, A.; Wang, W.; Wang, D.; Kröcher, O.; Prati, L., Selectivity Control in Palladium-Catalyzed Alcohol Oxidation through Selective Blocking of Active Sites. *J. Phys. Chem. C*, **2016**, *120* (26), 14027-14033. DOI: 10.1021/acs.jpcc.6b01549.
50. Villa, A.; Wang, D.; Veith, G. M.; Vindigni, F.; Prati, L., Sol immobilization technique: a delicate balance between activity, selectivity and stability of gold catalysts. *Catal. Sci. Technol.*, **2013**, *3* (11), 3036-3041. DOI: 10.1039/c3cy00260h.
51. Xia, H.; An, J.; Zhang, W., Aerobic Oxidation of 5-Hydroxymethylfurfural over Ag Nanoparticle Catalysts Stabilized by Polyvinylpyrrolidone with Different Molecular Weights. *Nanomaterials (Basel)*, **2020**, *10* (9), 1624. DOI: 10.3390/nano10091624.
52. Schrader, I.; Neumann, S.; Šilce, A.; Schmidt, F.; Azov, V.; Kunz, S., Asymmetric Heterogeneous Catalysis: Transfer of Molecular Principles to Nanoparticles by Ligand Functionalization. *ACS Catal.*, **2017**, *7* (6), 3979-3987. DOI: 10.1021/acscatal.7b00422.
53. Witte, P. T.; Berben, P. H.; Boland, S.; Boymans, E. H.; Vogt, D.; Geus, J. W.; Donkervoort, J. G., BASF NanoSelect™ Technology: Innovative Supported Pd- and Pt-based Catalysts for Selective Hydrogenation Reactions. *Top. Catal.*, **2012**, *55* (7-10), 505-511. DOI: 10.1007/s11244-012-9818-y.
54. Kwon, S. G.; Krylova, G.; Sumer, A.; Schwartz, M. M.; Bunel, E. E.; Marshall, C. L.; Chattopadhyay, S.; Lee, B.; Jellinek, J.; Shevchenko, E. V., Capping ligands as selectivity switchers in hydrogenation reactions. *Nano Lett.*, **2012**, *12* (10), 5382-5388. DOI: 10.1021/nl3027636.
55. Duran Pachon, L.; Yosef, I.; Markus, T. Z.; Naaman, R.; Avnir, D.; Rothenberg, G., Chiral imprinting of palladium with cinchona alkaloids. *Nat. Chem.*, **2009**, *1* (2), 160-164. DOI: 10.1038/nchem.180.
56. Neal, R. D.; Hughes, R. A.; Sapkota, P.; Ptasinska, S.; Neretina, S., Effect of Nanoparticle Ligands on 4-Nitrophenol Reduction: Reaction Rate, Induction Time, and Ligand Desorption. *ACS Catal.*, **2020**, *10* (17), 10040-10050. DOI: 10.1021/acscatal.0c02759.
57. Chu, C.; Huang, D.; Zhu, Q.; Stavitski, E.; Spies, J. A.; Pan, Z.; Mao, J.; Xin, H. L.; Schmuttenmaer, C. A.; Hu, S.; Kim, J.-H., Electronic Tuning of Metal Nanoparticles for Highly Efficient Photocatalytic Hydrogen Peroxide Production. *ACS Catal.*, **2018**, *9* (1), 626-631. DOI: 10.1021/acscatal.8b03738.
58. Vile, G.; Almora-Barrios, N.; Mitchell, S.; Lopez, N.; Perez-Ramirez, J., From the Lindlar catalyst to supported ligand-modified palladium nanoparticles: selectivity patterns and accessibility constraints in the continuous-flow three-phase hydrogenation

- of acetylenic compounds. *Chemistry*, **2014**, *20* (20), 5926-5937. DOI: 10.1002/chem.201304795.
59. Shen, H.; Deng, G.; Kaappa, S.; Tan, T.; Han, Y. Z.; Malola, S.; Lin, S. C.; Teo, B. K.; Hakkinen, H.; Zheng, N., Highly Robust but Surface-Active: An N-Heterocyclic Carbene-Stabilized Au<sub>25</sub> Nanocluster. *Angew. Chem. Int. Ed.*, **2019**, *58* (49), 17731-17735. DOI: 10.1002/anie.201908983.
60. Chen, G.; Xu, C.; Huang, X.; Ye, J.; Gu, L.; Li, G.; Tang, Z.; Wu, B.; Yang, H.; Zhao, Z.; Zhou, Z.; Fu, G.; Zheng, N., Interfacial electronic effects control the reaction selectivity of platinum catalysts. *Nat. Mater.*, **2016**, *15* (5), 564-569. DOI: 10.1038/nmat4555.
61. Šulce, A.; Flaherty, D. W.; Kunz, S., Kinetic analysis of the asymmetric hydrogenation of  $\beta$ -keto esters over  $\alpha$ -amino acid-functionalized Pt nanoparticles. *J. Catal.*, **2019**, *374*, 82-92. DOI: 10.1016/j.jcat.2019.04.020.
62. Albani, D.; Vilé, G.; Mitchell, S.; Witte, P. T.; Almora-Barrios, N.; Verel, R.; López, N.; Pérez-Ramírez, J., Ligand ordering determines the catalytic response of hybrid palladium nanoparticles in hydrogenation. *Catal. Sci. Technol.*, **2016**, *6* (6), 1621-1631. DOI: 10.1039/c5cy01921d.
63. Šulce, A.; Backenköhler, J.; Schrader, I.; Piane, M. D.; Müller, C.; Wark, A.; Ciacchi, L. C.; Azov, V.; Kunz, S., Ligand-functionalized Pt nanoparticles as asymmetric heterogeneous catalysts: molecular reaction control by ligand–reactant interactions. *Catal. Sci. Technol.*, **2018**, *8* (23), 6062-6075. DOI: 10.1039/c8cy01836g.
64. Irtem, E.; Arenas Esteban, D.; Duarte, M.; Choukroun, D.; Lee, S.; Ibáñez, M.; Bals, S.; Breugelmans, T., Ligand-Mode Directed Selectivity in Cu–Ag Core–Shell Based Gas Diffusion Electrodes for CO<sub>2</sub> Electroreduction. *ACS Catal.*, **2020**, *10* (22), 13468-13478. DOI: 10.1021/acscatal.0c03210.
65. Ernst, J. B.; Schwermann, C.; Yokota, G. I.; Tada, M.; Muratsugu, S.; Doltsinis, N. L.; Glorius, F., Molecular Adsorbates Switch on Heterogeneous Catalysis: Induction of Reactivity by N-Heterocyclic Carbenes. *J. Am. Chem. Soc.*, **2017**, *139* (27), 9144-9147. DOI: 10.1021/jacs.7b05112.
66. Cure, J.; Coppel, Y.; Dammak, T.; Fazzini, P. F.; Mlayah, A.; Chaudret, B.; Fau, P., Monitoring the coordination of amine ligands on silver nanoparticles using NMR and SERS. *Langmuir*, **2015**, *31* (4), 1362-1367. DOI: 10.1021/la504715f.
67. Witte, P. T.; Boland, S.; Kirby, F.; van Maanen, R.; Bleeker, B. F.; de Winter, D. A. M.; Post, J. A.; Geus, J. W.; Berben, P. H., NanoSelect Pd Catalysts: What Causes the High Selectivity of These Supported Colloidal Catalysts in Alkyne Semi-Hydrogenation? *ChemCatChem*, **2013**, *5* (2), 582-587. DOI: 10.1002/cctc.201200460.
68. Fiorio, J. L.; Barbosa, E. C. M.; Kikuchi, D. K.; Camargo, P. H. C.; Rudolph, M.; Hashmi, A. S. K.; Rossi, L. M., Piperazine-promoted gold-catalyzed hydrogenation: the influence of capping ligands. *Catal. Sci. Technol.*, **2020**, *10* (7), 1996-2003. DOI: 10.1039/c9cy02016k.
69. Wu, B.; Huang, H.; Yang, J.; Zheng, N.; Fu, G., Selective hydrogenation of alpha, beta-unsaturated aldehydes catalyzed by amine-capped platinum-cobalt nanocrystals. *Angew. Chem. Int. Ed.*, **2012**, *51* (14), 3440-3443. DOI: 10.1002/anie.201108593.
70. Cano, I.; Chapman, A. M.; Urakawa, A.; van Leeuwen, P. W., Air-stable gold nanoparticles ligated by secondary phosphine oxides for the chemoselective hydrogenation of aldehydes: crucial role of the ligand. *J. Am. Chem. Soc.*, **2014**, *136* (6), 2520-2528. DOI: 10.1021/ja411202h.
71. Ortuño, M. A.; López, N., Creating Cavities at Palladium–Phosphine Interfaces for Enhanced Selectivity in Heterogeneous Biomass Conversion. *ACS Catal.*, **2018**, *8* (7), 6138-6145. DOI: 10.1021/acscatal.8b01302.

72. Chatterjee, A.; Jensen, V. R., A Heterogeneous Catalyst for the Transformation of Fatty Acids to  $\alpha$ -Olefins. *ACS Catal.*, **2017**, *7* (4), 2543-2547. DOI: 10.1021/acscatal.6b03460.
73. Guo, M.; Li, H.; Ren, Y.; Ren, X.; Yang, Q.; Li, C., Improving Catalytic Hydrogenation Performance of Pd Nanoparticles by Electronic Modulation Using Phosphine Ligands. *ACS Catal.*, **2018**, *8* (7), 6476-6485. DOI: 10.1021/acscatal.8b00872.
74. Liu, Y.; McCue, A. J.; Miao, C.; Feng, J.; Li, D.; Anderson, J. A., Palladium phosphide nanoparticles as highly selective catalysts for the selective hydrogenation of acetylene. *J. Catal.*, **2018**, *364*, 406-414. DOI: 10.1016/j.jcat.2018.06.001.
75. Rafter, E.; Gutmann, T.; Löw, F.; Buntkowsky, G.; Philippot, K.; Chaudret, B.; van Leeuwen, P. W. N. M., Secondary phosphineoxides as pre-ligands for nanoparticle stabilization. *Catal. Sci. Technol.*, **2013**, *3* (3), 595-599. DOI: 10.1039/c2cy20683h.
76. Fedorov, A.; Liu, H. J.; Lo, H. K.; Coperet, C., Silica-Supported Cu Nanoparticle Catalysts for Alkyne Semihydrogenation: Effect of Ligands on Rates and Selectivity. *J. Am. Chem. Soc.*, **2016**, *138* (50), 16502-16507. DOI: 10.1021/jacs.6b10817.
77. McCue, A. J.; McKenna, F.-M.; Anderson, J. A., Triphenylphosphine: a ligand for heterogeneous catalysis too? Selectivity enhancement in acetylene hydrogenation over modified Pd/TiO<sub>2</sub> catalyst. *Catal. Sci. Technol.*, **2015**, *5* (4), 2449-2459. DOI: 10.1039/c5cy00065c.
78. Snelders, D. J. M.; Yan, N.; Gan, W.; Laurenczy, G.; Dyson, P. J., Tuning the Chemoselectivity of Rh Nanoparticle Catalysts by Site-Selective Poisoning with Phosphine Ligands: The Hydrogenation of Functionalized Aromatic Compounds. *ACS Catal.*, **2012**, *2* (2), 201-207. DOI: 10.1021/cs200575r.
79. Rogers, S. M.; Dimitratos, N.; Jones, W.; Bowker, M.; Kanaras, A. G.; Wells, P. P.; Catlow, C. R.; Parker, S. F., The adsorbed state of a thiol on palladium nanoparticles. *Phys. Chem. Chem. Phys.*, **2016**, *18* (26), 17265-17271. DOI: 10.1039/c6cp00957c.
80. Khasar, K. R.; Schwartz, D. K.; Medlin, J. W., Control of metal catalyst selectivity through specific noncovalent molecular interactions. *J. Am. Chem. Soc.*, **2014**, *136* (1), 520-526. DOI: 10.1021/ja411973p.
81. Marshall, S. T.; O'Brien, M.; Oetter, B.; Corpuz, A.; Richards, R. M.; Schwartz, D. K.; Medlin, J. W., Controlled selectivity for palladium catalysts using self-assembled monolayers. *Nat. Mater.*, **2010**, *9* (10), 853-858. DOI: 10.1038/nmat2849.
82. Schoenbaum, C. A.; Schwartz, D. K.; Medlin, J. W., Controlling surface crowding on a Pd catalyst with thiolate self-assembled monolayers. *J. Catal.*, **2013**, *303*, 92-99. DOI: 10.1016/j.jcat.2013.03.012.
83. Schoenbaum, C. A.; Schwartz, D. K.; Medlin, J. W., Controlling the surface environment of heterogeneous catalysts using self-assembled monolayers. *Acc. Chem. Res.*, **2014**, *47* (4), 1438-1445. DOI: 10.1021/ar500029y.
84. Pang, S. H.; Schoenbaum, C. A.; Schwartz, D. K.; Medlin, J. W., Directing reaction pathways by catalyst active-site selection using self-assembled monolayers. *Nat. Commun.*, **2013**, *4*, 2448. DOI: 10.1038/ncomms3448.
85. Shang, H.; Wallentine, S. K.; Hofmann, D. M.; Zhu, Q.; Murphy, C. J.; Baker, L. R., Effect of surface ligands on gold nanocatalysts for CO<sub>2</sub> reduction. *Chem. Sci.*, **2020**, *11* (45), 12298-12306. DOI: 10.1039/d0sc05089j.
86. Pang, S. H.; Schoenbaum, C. A.; Schwartz, D. K.; Medlin, J. W., Effects of Thiol Modifiers on the Kinetics of Furfural Hydrogenation over Pd Catalysts. *ACS Catal.*, **2014**, *4* (9), 3123-3131. DOI: 10.1021/cs500598y.
87. Taguchi, T.; Isozaki, K.; Miki, K., Enhanced catalytic activity of self-assembled-monolayer-capped gold nanoparticles. *Adv. Mater.*, **2012**, *24* (48), 6462-6467. DOI: 10.1002/adma.201202979.



88. McKenna, F. M.; Wells, R. P.; Anderson, J. A., Enhanced selectivity in acetylene hydrogenation by ligand modified Pd/TiO<sub>2</sub> catalysts. *Chem. Commun.*, **2011**, 47 (8), 2351-2353. DOI: 10.1039/C0CC01742F.
89. Love, J. C.; Wolfe, D. B.; Haasch, R.; Chabynyc, M. L.; Paul, K. E.; Whitesides, G. M.; Nuzzo, R. G., Formation and structure of self-assembled monolayers of alkanethiolates on palladium. *J. Am. Chem. Soc.*, **2003**, 125 (9), 2597-2609. DOI: 10.1021/ja028692+.
90. Weng, Z.; Zaera, F., Increase in Activity and Selectivity in Catalysis via Surface Modification with Self-Assembled Monolayers. *J. Phys. Chem. C*, **2014**, 118 (7), 3672-3679. DOI: 10.1021/jp412364d.
91. Altmann, L.; Kunz, S.; Bäumer, M., Influence of Organic Amino and Thiol Ligands on the Geometric and Electronic Surface Properties of Colloidally Prepared Platinum Nanoparticles. *J. Phys. Chem. C*, **2014**, 118 (17), 8925-8932. DOI: 10.1021/jp4116707.
92. Huang, L.; Subramanian, R.; Wang, J.; Kwon Oh, J.; Ye, Z., Ligand screening for palladium nanocatalysts towards selective hydrogenation of alkynes. *Mol. Catal.*, **2020**, 488, 110923. DOI: 10.1016/j.mcat.2020.110923.
93. Makosch, M.; Lin, W.-I.; Bumbálek, V.; Sá, J.; Medlin, J. W.; Hungerbühler, K.; van Bokhoven, J. A., Organic Thiol Modified Pt/TiO<sub>2</sub> Catalysts to Control Chemoselective Hydrogenation of Substituted Nitroarenes. *ACS Catal.*, **2012**, 2 (10), 2079-2081. DOI: 10.1021/cs300378p.
94. Sadeghmoghaddam, E.; Gu, H.; Shon, Y. S., Pd Nanoparticle-Catalyzed Isomerization vs Hydrogenation of Allyl Alcohol: Solvent-Dependent Regioselectivity. *ACS Catal.*, **2012**, 2 (9), 1838-1845. DOI: 10.1021/cs300270d.
95. Centrone, A.; Penzo, E.; Sharma, M.; Myerson, J. W.; Jackson, A. M.; Marzari, N.; Stellacci, F., The role of nanostructure in the wetting behavior of mixed-monolayer-protected metal nanoparticles. *Proc. Natl. Acad. Sci. U S A*, **2008**, 105 (29), 9886-9891. DOI: 10.1073/pnas.0803929105.
96. Haider, P.; Urakawa, A.; Schmidt, E.; Baiker, A., Selective blocking of active sites on supported gold catalysts by adsorbed thiols and its effect on the catalytic behavior: A combined experimental and theoretical study. *J. Mol. Catal. A Chem.*, **2009**, 305 (1-2), 161-169. DOI: 10.1016/j.molcata.2009.02.025.
97. Albani, D.; Shahrokhi, M.; Chen, Z.; Mitchell, S.; Hauert, R.; Lopez, N.; Perez-Ramirez, J., Selective ensembles in supported palladium sulfide nanoparticles for alkyne semi-hydrogenation. *Nat. Commun.*, **2018**, 9 (1), 2634. DOI: 10.1038/s41467-018-05052-4.
98. McCue, A. J.; Guerrero-Ruiz, A.; Ramirez-Barria, C.; Rodríguez-Ramos, I.; Anderson, J. A., Selective hydrogenation of mixed alkyne/alkene streams at elevated pressure over a palladium sulfide catalyst. *J. Catal.*, **2017**, 355, 40-52. DOI: 10.1016/j.jcat.2017.09.004.
99. Khsar, K. R.; Schwartz, D. K.; Medlin, J. W., Selective Hydrogenation of Polyunsaturated Fatty Acids Using Alkanethiol Self-Assembled Monolayer-Coated Pd/Al<sub>2</sub>O<sub>3</sub> Catalysts. *ACS Catal.*, **2013**, 3 (9), 2041-2044. DOI: 10.1021/cs4004563.
100. McKenna, F.-M.; Anderson, J. A., Selectivity enhancement in acetylene hydrogenation over diphenyl sulphide-modified Pd/TiO<sub>2</sub> catalysts. *J. Catal.*, **2011**, 281 (2), 231-240. DOI: 10.1016/j.jcat.2011.05.003.
101. Zhao, X.; Zhou, L.; Zhang, W.; Hu, C.; Dai, L.; Ren, L.; Wu, B.; Fu, G.; Zheng, N., Thiol Treatment Creates Selective Palladium Catalysts for Semihydrogenation of Internal Alkynes. *Chem*, **2018**, 4 (5), 1080-1091. DOI: 10.1016/j.chempr.2018.02.011.

102. F. de L. e Freitas, L.; Puértolas, B.; Zhang, J.; Wang, B.; Hoffman, A. S.; Bare, S. R.; Pérez-Ramírez, J.; Medlin, J. W.; Nikolla, E., Tunable Catalytic Performance of Palladium Nanoparticles for H<sub>2</sub>O<sub>2</sub> Direct Synthesis via Surface-Bound Ligands. *ACS Catal.*, **2020**, *10* (9), 5202-5207. DOI: 10.1021/acscatal.0c01517.
103. Andryushechkin, B. V.; Pavlova, T. V.; Eltsov, K. N., Adsorption of halogens on metal surfaces. *Surf. Sci. Rep.*, **2018**, *73* (3), 83-115. DOI: 10.1016/j.surfrep.2018.03.001.
104. Seshu Babu, N.; Lingaiah, N.; Sai Prasad, P. S., Characterization and reactivity of Al<sub>2</sub>O<sub>3</sub> supported Pd-Ni bimetallic catalysts for hydrodechlorination of chlorobenzene. *Appl. Catal. B.*, **2012**, *111-112*, 309-316. DOI: 10.1016/j.apcatb.2011.10.013.
105. Ma, X.; Liu, S.; Liu, Y.; Gu, G.; Xia, C., Comparative study on catalytic hydrodehalogenation of halogenated aromatic compounds over Pd/C and Raney Ni catalysts. *Sci. Rep.*, **2016**, *6*, 25068. DOI: 10.1038/srep25068.
106. Wu, D.; Zhang, S.; Hernández, W. Y.; Baaziz, W.; Ersen, O.; Marinova, M.; Khodakov, A. Y.; Ordonsky, V. V., Dual Metal–Acid Pd-Br Catalyst for Selective Hydrodeoxygenation of 5-Hydroxymethylfurfural (HMF) to 2,5-Dimethylfuran at Ambient Temperature. *ACS Catal.*, **2020**, *11* (1), 19-30. DOI: 10.1021/acscatal.0c03955.
107. Roman, T.; Gossenberger, F.; Forster-Tonigold, K.; Gross, A., Halide adsorption on close-packed metal electrodes. *Phys. Chem. Chem. Phys.*, **2014**, *16* (27), 13630-13634. DOI: 10.1039/c4cp00237g.
108. Wu, D.; Hernández, W. Y.; Zhang, S.; Vovk, E. I.; Zhou, X.; Yang, Y.; Khodakov, A. Y.; Ordonsky, V. V., In Situ Generation of Brønsted Acidity in the Pd-I Bifunctional Catalysts for Selective Reductive Etherification of Carbonyl Compounds under Mild Conditions. *ACS Catal.*, **2019**, *9* (4), 2940-2948. DOI: 10.1021/acscatal.8b04925.
109. Wu, D.; Wang, Q.; Safonova, O. V.; Peron, D. V.; Zhou, W.; Yan, Z.; Marinova, M.; Khodakov, A. Y.; Ordonsky, V. V., Lignin Compounds to Monoaromatics: Selective Cleavage of C-O Bonds over a Brominated Ruthenium Catalyst. *Angew. Chem. Int. Ed.*, **2021**, *60* (22), 12513-12523. DOI: 10.1002/anie.202101325.
110. Bjork, J.; Hanke, F.; Stafstrom, S., Mechanisms of halogen-based covalent self-assembly on metal surfaces. *J. Am. Chem. Soc.*, **2013**, *135* (15), 5768-5775. DOI: 10.1021/ja400304b.
111. Harris, J. W.; Herron, J. A.; DeWilde, J. F.; Bhan, A., Molecular characteristics governing chlorine deposition and removal on promoted Ag catalysts during ethylene epoxidation. *J. Catal.*, **2019**, *377*, 378-388. DOI: 10.1016/j.jcat.2019.07.043.
112. Ramirez, A.; Hueso, J. L.; Suarez, H.; Mallada, R.; Ibarra, A.; Irusta, S.; Santamaria, J., A Nanoarchitecture Based on Silver and Copper Oxide with an Exceptional Response in the Chlorine-Promoted Epoxidation of Ethylene. *Angew. Chem. Int. Ed.*, **2016**, *55* (37), 11158-11161. DOI: 10.1002/anie.201603886.
113. Zhao, Y.; Ling, T.; Chen, S.; Jin, B.; Vasileff, A.; Jiao, Y.; Song, L.; Luo, J.; Qiao, S. Z., Non-metal Single-Iodine-Atom Electrocatalysts for the Hydrogen Evolution Reaction. *Angew. Chem. Int. Ed.*, **2019**, *58* (35), 12252-12257. DOI: 10.1002/anie.201905554.
114. Rocha, T. C. R.; Hävecker, M.; Knop-Gericke, A.; Schlögl, R., Promoters in heterogeneous catalysis: The role of Cl on ethylene epoxidation over Ag. *J. Catal.*, **2014**, *312*, 12-16. DOI: 10.1016/j.jcat.2014.01.002.
115. Choudhary, V.; Samanta, C., Role of chloride or bromide anions and protons for promoting the selective oxidation of H<sub>2</sub> by O<sub>2</sub> to H<sub>2</sub>O<sub>2</sub> over supported Pd catalysts in an aqueous medium. *J. Catal.*, **2006**, *238* (1), 28-38. DOI: 10.1016/j.jcat.2005.11.024.
116. Meng, Q.; Hou, M.; Liu, H.; Song, J.; Han, B., Synthesis of ketones from biomass-derived feedstock. *Nat. Commun.*, **2017**, *8*, 14190. DOI: 10.1038/ncomms14190.

117. Oliveira, V.; Cremer, D., Transition from metal-ligand bonding to halogen bonding involving a metal as halogen acceptor a study of Cu, Ag, Au, Pt, and Hg complexes. *Chem. Phys. Lett.*, **2017**, *681*, 56-63. DOI: 10.1016/j.cplett.2017.05.045.
118. Zhu, Q.; Wang, S.-q., Trends and Regularities for Halogen Adsorption on Various Metal Surfaces. *J. Electrochem. Soc.*, **2016**, *163* (9), H796-H808. DOI: 10.1149/2.0821609jes.
119. Duan, H.; Wang, D.; Li, Y., Green chemistry for nanoparticle synthesis. *Chem. Soc. Rev.*, **2015**, *44* (16), 5778-5792. DOI: 10.1039/c4cs00363b.
120. Rodrigues, T. S.; da Silva, A. G. M.; Camargo, P. H. C., Nanocatalysis by noble metal nanoparticles: controlled synthesis for the optimization and understanding of activities. *J. Mater. Chem. A*, **2019**, *7* (11), 5857-5874. DOI: 10.1039/c9ta00074g.
121. Favier, I.; Pla, D.; Gomez, M., Palladium Nanoparticles in Polyols: Synthesis, Catalytic Couplings, and Hydrogenations. *Chem. Rev.*, **2020**, *120* (2), 1146-1183. DOI: 10.1021/acs.chemrev.9b00204.
122. Gu, J.; Zhang, Y. W.; Tao, F. F., Shape control of bimetallic nanocatalysts through well-designed colloidal chemistry approaches. *Chem. Soc. Rev.*, **2012**, *41* (24), 8050-8065. DOI: 10.1039/c2cs35184f.
123. Pankhurst, J. R.; Iyengar, P.; Loiudice, A.; Mensi, M.; Buonsanti, R., Metal–ligand bond strength determines the fate of organic ligands on the catalyst surface during the electrochemical CO<sub>2</sub> reduction reaction. *Chem. Sci.*, **2020**, *11* (34), 9296-9302. DOI: 10.1039/d0sc03061a.
124. Astruc, D.; Lu, F.; Aranzaes, J. R., Nanoparticles as recyclable catalysts: the frontier between homogeneous and heterogeneous catalysis. *Angew. Chem. Int. Ed.*, **2005**, *44* (48), 7852-7872. DOI: 10.1002/anie.200500766.
125. Sá, J.; Medlin, J. W., On-the-fly Catalyst Modification: Strategy to Improve Catalytic Processes Selectivity and Understanding. *ChemCatChem*, **2019**, *11* (15), 3355-3365. DOI: 10.1002/cctc.201900770.
126. Ortuño, M. A.; López, N., Reaction mechanisms at the homogeneous–heterogeneous frontier: insights from first-principles studies on ligand-decorated metal nanoparticles. *Catal. Sci. Technol.*, **2019**, *9* (19), 5173-5185. DOI: 10.1039/c9cy01351b.
127. Guntern, Y. T.; Okatenko, V.; Pankhurst, J.; Varandili, S. B.; Iyengar, P.; Koolen, C.; Stoian, D.; Vavra, J.; Buonsanti, R., Colloidal Nanocrystals as Electrocatalysts with Tunable Activity and Selectivity. *ACS Catal.*, **2021**, *11* (3), 1248-1295. DOI: 10.1021/acscatal.0c04403.
128. Collins, G.; Davitt, F.; O'Dwyer, C.; Holmes, J. D., Comparing Thermal and Chemical Removal of Nanoparticle Stabilizing Ligands: Effect on Catalytic Activity and Stability. *ACS Appl. Nano Mater.*, **2018**, *1* (12), 7129-7138. DOI: 10.1021/acsanm.8b02019.
129. Bachar, O.; Meirovich, M. M.; Kurzion, R.; Yehezkeili, O., In vivo and in vitro protein mediated synthesis of palladium nanoparticles for hydrogenation reactions. *Chem. Commun.*, **2020**, *56* (76), 11211-11214. DOI: 10.1039/d0cc04812g.
130. Farshad, M.; Suvlu, D.; Rasaiah, J. C., Ligand-Mediated Nanocluster Formation with Classical and Autocatalytic Growth. *J. Phys. Chem. C*, **2019**, *123* (49), 29954-29963. DOI: 10.1021/acs.jpcc.9b07683.
131. Shi, Y.; Lyu, Z.; Zhao, M.; Chen, R.; Nguyen, Q. N.; Xia, Y., Noble-Metal Nanocrystals with Controlled Shapes for Catalytic and Electrocatalytic Applications. *Chem. Rev.*, **2021**, *121* (2), 649-735. DOI: 10.1021/acs.chemrev.0c00454.
132. Yang, T. H.; Shi, Y.; Janssen, A.; Xia, Y., Surface Capping Agents and Their Roles in Shape-Controlled Synthesis of Colloidal Metal Nanocrystals. *Angew. Chem. Int. Ed.*, **2020**, *59* (36), 15378-15401. DOI: 10.1002/anie.201911135.

133. Huo, D.; Kim, M. J.; Lyu, Z.; Shi, Y.; Wiley, B. J.; Xia, Y., One-Dimensional Metal Nanostructures: From Colloidal Syntheses to Applications. *Chem. Rev.*, **2019**, *119* (15), 8972-9073. DOI: 10.1021/acs.chemrev.8b00745.
134. Scanlon, M. D.; Peljo, P.; Mendez, M. A.; Smirnov, E.; Girault, H. H., Charging and discharging at the nanoscale: Fermi level equilibration of metallic nanoparticles. *Chem. Sci.*, **2015**, *6* (5), 2705-2720. DOI: 10.1039/c5sc00461f.
135. Fogg, D. E.; dos Santos, E. N., Tandem catalysis: a taxonomy and illustrative review. *Coord. Chem. Rev.*, **2004**, *248* (21-24), 2365-2379. DOI: 10.1016/j.ccr.2004.05.012.
136. Canlas, C. P.; Lu, J.; Ray, N. A.; Grosso-Giordano, N. A.; Lee, S.; Elam, J. W.; Winans, R. E.; Van Duyne, R. P.; Stair, P. C.; Notestein, J. M., Shape-selective sieving layers on an oxide catalyst surface. *Nat. Chem.*, **2012**, *4* (12), 1030-1036. DOI: 10.1038/nchem.1477.
137. Teschner, D.; Borsodi, J.; Wootsch, A.; Revay, Z.; Havecker, M.; Knop-Gericke, A.; Jackson, S. D.; Schlögl, R., The roles of subsurface carbon and hydrogen in palladium-catalyzed alkyne hydrogenation. *Science*, **2008**, *320* (5872), 86-89. DOI: 10.1126/science.1155200.
138. Chan, C. W.; Mahadi, A. H.; Li, M. M.; Corbos, E. C.; Tang, C.; Jones, G.; Kuo, W. C.; Cookson, J.; Brown, C. M.; Bishop, P. T.; Tsang, S. C., Interstitial modification of palladium nanoparticles with boron atoms as a green catalyst for selective hydrogenation. *Nat. Commun.*, **2014**, *5*, 5787. DOI: 10.1038/ncomms6787.
139. Wei, Z.; Yao, Z.; Zhou, Q.; Zhuang, G.; Zhong, X.; Deng, S.; Li, X.; Wang, J., Optimizing Alkyne Hydrogenation Performance of Pd on Carbon in Situ Decorated with Oxygen-Deficient TiO<sub>2</sub> by Integrating the Reaction and Diffusion. *ACS Catal.*, **2019**, *9* (12), 10656-10667. DOI: 10.1021/acscatal.9b03300.
140. Tang, Y.; Dong, K.; Wang, S.; Sun, Q.; Meng, X.; Xiao, F.-S., Boosting the hydrolytic stability of phosphite ligand in hydroformylation by the construction of superhydrophobic porous framework. *Mol. Catal.*, **2019**, *474*. DOI: 10.1016/j.mcat.2019.110408.
141. Jin, Z.; Wang, L.; Zuidema, E.; Mondal, K.; Zhang, M.; Zhang, J.; Wang, C.; Meng, X.; Yang, H.; Mesters, C.; Xiao, F. S., Hydrophobic zeolite modification for in situ peroxide formation in methane oxidation to methanol. *Science*, **2020**, *367* (6474), 193-197. DOI: 10.1126/science.aaw1108.
142. Wang, C.; Liu, Z.; Wang, L.; Dong, X.; Zhang, J.; Wang, G.; Han, S.; Meng, X.; Zheng, A.; Xiao, F.-S., Importance of Zeolite Wettability for Selective Hydrogenation of Furfural over Pd@Zeolite Catalysts. *ACS Catal.*, **2017**, *8* (1), 474-481. DOI: 10.1021/acscatal.7b03443.
143. Luneau, M.; Lim, J. S.; Patel, D. A.; Sykes, E. C. H.; Friend, C. M.; Sautet, P., Guidelines to Achieving High Selectivity for the Hydrogenation of alpha, beta-Unsaturated Aldehydes with Bimetallic and Dilute Alloy Catalysts: A Review. *Chem. Rev.*, **2020**, *120* (23), 12834-12872. DOI: 10.1021/acs.chemrev.0c00582.
144. Lari, G. M.; Puertolas, B.; Shahrokhi, M.; Lopez, N.; Perez-Ramirez, J., Hybrid Palladium Nanoparticles for Direct Hydrogen Peroxide Synthesis: The Key Role of the Ligand. *Angew. Chem. Int. Ed.*, **2017**, *56* (7), 1775-1779. DOI: 10.1002/anie.201610552.
145. Katz, A.; Davis, M. E., Molecular imprinting of bulk, microporous silica. *Nature*, **2000**, *403* (6767), 286-289. DOI: 10.1038/35002032.
146. Chen, L.; Wang, X.; Lu, W.; Wu, X.; Li, J., Molecular imprinting: perspectives and applications. *Chem. Soc. Rev.*, **2016**, *45* (8), 2137-2211. DOI: 10.1039/c6cs00061d.
147. Wu, D.; Baaziz, W.; Gu, B.; Marinova, M.; Hernandez, W. Y.; Zhou, W. J.; Vovk, E. I.; Ersen, O.; Safonova, O. V.; Addad, A.; Nuns, N.; Khodakov, A. Y.; Ordonsky, V. V.,

Surface molecular imprinting over supported metal catalysts for size-dependent selective hydrogenation reactions. *Nat. Catal.*, **2021**, *4* (7), 595-606. DOI: 10.1038/s41929-021-00649-3.

148. Francis, J.; Guillon, E.; Bats, N.; Pichon, C.; Corma, A.; Simon, L. J., Design of improved hydrocracking catalysts by increasing the proximity between acid and metallic sites. *Appl. Catal. A: Gen.*, **2011**, *409-410*, 140-147. DOI: 10.1016/j.apcata.2011.09.040.

149. Ju, C.; Li, M.; Fang, Y.; Tan, T., Efficient hydro-deoxygenation of lignin derived phenolic compounds over bifunctional catalysts with optimized acid/metal interactions. *Green Chem.*, **2018**, *20* (19), 4492-4499. DOI: 10.1039/c8gc01960f.

150. Guisnet, M., "Ideal" bifunctional catalysis over Pt-acid zeolites. *Catal. Today*, **2013**, *218-219*, 123-134. DOI: 10.1016/j.cattod.2013.04.028.

151. Zecevic, J.; Vanbutsele, G.; de Jong, K. P.; Martens, J. A., Nanoscale intimacy in bifunctional catalysts for selective conversion of hydrocarbons. *Nature*, **2015**, *528* (7581), 245-248. DOI: 10.1038/nature16173.

152. Liu, Q.; Yang, X.; Li, L.; Miao, S.; Li, Y.; Li, Y.; Wang, X.; Huang, Y.; Zhang, T., Direct catalytic hydrogenation of CO<sub>2</sub> to formate over a Schiff-base-mediated gold nanocatalyst. *Nat. Commun.*, **2017**, *8* (1), 1407. DOI: 10.1038/s41467-017-01673-3.

153. Liu, Q.; Yang, X.; Huang, Y.; Xu, S.; Su, X.; Pan, X.; Xu, J.; Wang, A.; Liang, C.; Wang, X.; Zhang, T., A Schiff base modified gold catalyst for green and efficient H<sub>2</sub> production from formic acid. *Energy Environ. Sci.*, **2015**, *8* (11), 3204-3207. DOI: 10.1039/c5ee02506k.

154. Jin, Z.; Yi, X.; Wang, L.; Xu, S.; Wang, C.; Wu, Q.; Wang, L.; Zheng, A.; Xiao, F.-S., Metal-acid interfaces enveloped in zeolite crystals for cascade biomass hydrodeoxygenation. *Appl. Catal. B*, **2019**, *254*, 560-568. DOI: 10.1016/j.apcatb.2019.05.022.

155. Zhong, R.-Y.; Sun, K.-Q.; Hong, Y.-C.; Xu, B.-Q., Impacts of Organic Stabilizers on Catalysis of Au Nanoparticles from Colloidal Preparation. *ACS Catal.*, **2014**, *4* (11), 3982-3993. DOI: 10.1021/cs501161c.

156. Zhao, Y.; Baeza, J. A.; Koteswara Rao, N.; Calvo, L.; Gilarranz, M. A.; Li, Y. D.; Lefferts, L., Unsupported PVA- and PVP-stabilized Pd nanoparticles as catalyst for nitrite hydrogenation in aqueous phase. *J. Catal.*, **2014**, *318*, 162-169. DOI: 10.1016/j.jcat.2014.07.011.

157. Zhong, R.-Y.; Yan, X.-H.; Gao, Z.-K.; Zhang, R.-J.; Xu, B.-Q., Stabilizer substitution and its effect on the hydrogenation catalysis by Au nanoparticles from colloidal synthesis. *Catal. Sci. Technol.*, **2013**, *3* (11), 3013-3019. DOI: 10.1039/c3cy00308f.

158. Albani, D.; Li, Q.; Vilé, G.; Mitchell, S.; Almora-Barrios, N.; Witte, P. T.; López, N.; Pérez-Ramírez, J., Interfacial acidity in ligand-modified ruthenium nanoparticles boosts the hydrogenation of levulinic acid to gamma-valerolactone. *Green Chem.*, **2017**, *19* (10), 2361-2370. DOI: 10.1039/c6gc02586b.

159. Schrader, I.; Warneke, J.; Backenkohler, J.; Kunz, S., Functionalization of platinum nanoparticles with L-proline: simultaneous enhancements of catalytic activity and selectivity. *J. Am. Chem. Soc.*, **2015**, *137* (2), 905-912. DOI: 10.1021/ja511349p.

160. Jeong, H.; Kim, C.; Yang, S.; Lee, H., Selective hydrogenation of furanic aldehydes using Ni nanoparticle catalysts capped with organic molecules. *J. Catal.*, **2016**, *344*, 609-615. DOI: 10.1016/j.jcat.2016.11.002.

161. Yang, Y.; Li, S.; Xie, C.; Liu, H.; Wang, Y.; Mei, Q.; Liu, H.; Han, B., Ethylenediamine promoted the hydrogenative coupling of nitroarenes over Ni/C catalyst. *Chin. Chem. Lett.*, **2019**, *30* (1), 203-206. DOI: 10.1016/j.ccllet.2018.04.006.

162. Šulce, A.; Mitschke, N.; Azov, V.; Kunz, S., Molecular Insights into the Ligand - Reactant Interactions of Pt Nanoparticles Functionalized with  $\alpha$ -Amino Acids as Asymmetric Catalysts for  $\beta$ -Keto Esters. *ChemCatChem* **2019**, *11* (11), 2732-2742. DOI: 10.1002/cctc.201900238.
163. Liu, H.; Mei, Q.; Li, S.; Yang, Y.; Wang, Y.; Liu, H.; Zheng, L.; An, P.; Zhang, J.; Han, B., Selective hydrogenation of unsaturated aldehydes over Pt nanoparticles promoted by the cooperation of steric and electronic effects. *Chem. Commun.*, **2018**, *54* (8), 908-911. DOI: 10.1039/c7cc08942b.
164. Fiorio, J. L.; López, N.; Rossi, L. M., Gold-Ligand-Catalyzed Selective Hydrogenation of Alkynes into cis-Alkenes via H<sub>2</sub> Heterolytic Activation by Frustrated Lewis Pairs. *ACS Catal.*, **2017**, *7* (4), 2973-2980. DOI: 10.1021/acscatal.6b03441.
165. Huang, L.; Hu, K.; Ye, G.; Ye, Z., Highly selective semi-hydrogenation of alkynes with a Pd nanocatalyst modified with sulfide-based solid-phase ligands. *Mol. Catal.*, **2021**, *506*, 111535. DOI: 10.1016/j.mcat.2021.111535.
166. Zhang, Q.; Su, C.; Cen, J.; Feng, F.; Ma, L.; Lu, C.; Li, X., The Modification of Diphenyl Sulfide to Pd/C Catalyst and Its Application in Selective Hydrogenation of p-Chloronitrobenzene. *Chin. J. Chem. Eng.*, **2014**, *22* (10), 1111-1116. DOI: 10.1016/j.cjche.2014.08.007.
167. Priyadarshini, P.; Ricciardulli, T.; Adams, J. S.; Yun, Y. S.; Flaherty, D. W., Effects of bromide adsorption on the direct synthesis of H<sub>2</sub>O<sub>2</sub> on Pd nanoparticles: Formation rates, selectivities, and apparent barriers at steady-state. *J. Catal.*, **2021**, *399*, 24-40. DOI: 10.1016/j.jcat.2021.04.020.
168. Ma, W.; Xie, S.; Liu, T.; Fan, Q.; Ye, J.; Sun, F.; Jiang, Z.; Zhang, Q.; Cheng, J.; Wang, Y., Electrocatalytic reduction of CO<sub>2</sub> to ethylene and ethanol through hydrogen-assisted C-C coupling over fluorine-modified copper. *Nat. Catal.*, **2020**, *3* (6), 478-487. DOI: 10.1038/s41929-020-0450-0.
169. Li, M.; Ma, Y.; Chen, J.; Lawrence, R.; Luo, W.; Sacchi, M.; Jiang, W.; Yang, J., Residual Chlorine Induced Cationic Active Species on a Porous Copper Electrocatalyst for Highly Stable Electrochemical CO<sub>2</sub> Reduction to C<sub>2</sub>. *Angew. Chem. Int. Ed.*, **2021**, *60* (20), 11487-11493. DOI: 10.1002/anie.202102606.
170. Li, H.; Liu, T.; Wei, P.; Lin, L.; Gao, D.; Wang, G.; Bao, X., High-Rate CO<sub>2</sub> Electroreduction to C<sub>2</sub><sup>+</sup> Products over a Copper-Copper Iodide Catalyst. *Angew. Chem. Int. Ed.*, **2021**, *60* (26), 14329-14333. DOI: 10.1002/anie.202102657.
171. Fievet, F.; Ammar-Merah, S.; Brayner, R.; Chau, F.; Giraud, M.; Mammeri, F.; Peron, J.; Piquemal, J. Y.; Sicard, L.; Viau, G., The polyol process: a unique method for easy access to metal nanoparticles with tailored sizes, shapes and compositions. *Chem. Soc. Rev.*, **2018**, *47* (14), 5187-5233. DOI: 10.1039/c7cs00777a.
172. Lu, Y.; Chen, W., Sub-nanometre sized metal clusters: from synthetic challenges to the unique property discoveries. *Chem. Soc. Rev.*, **2012**, *41* (9), 3594-3623. DOI: 10.1039/c2cs15325d.
173. Duan, H.; Wang, D.; Li, Y., Green chemistry for nanoparticle synthesis. *Chem. Soc. Rev.*, **2015**, *44* (16), 5778-5792. DOI: 10.1039/c4cs00363b.
174. Yang, T. H.; Shi, Y.; Janssen, A.; Xia, Y., Surface Capping Agents and Their Roles in Shape-Controlled Synthesis of Colloidal Metal Nanocrystals. *Angew. Chem. Int. Ed.*, **2020**, *59* (36), 15378-15401. DOI: 10.1002/anie.201911135.